The impact of V2X on battery degradation

A quantitative review

Linders, Koen; Jenu, Samppa; Hentunen, Ari; Chandra Mouli, Gautham Ram

DOI
10.1016/j.jpowsour.2025.238482

Publication date
2025

Document Version
Final published version

Published in
Journal of Power Sources

Journal of Power Sources 660 (2025) 238482

Contents lists available at ScienceDirect

Journal of Power Sources

journal homepage: www.elsevier.com/locate/jpowsour

Review article

The impact of V2X on battery degradation: A quantitative review

Koen Linders [a,*], Samppa Jenu [b], Ari Hentunen [b], Gautham Ram Chandra Mouli [a,*]

[a] Delft University of Technology, Mekelweg 5, 2628CD, Delft, The Netherlands
[b] VTT Technical Research Centre of Finland Ltd, Maarintie 3, 02150, Espoo, Finland

GRAPHICAL ABSTRACT

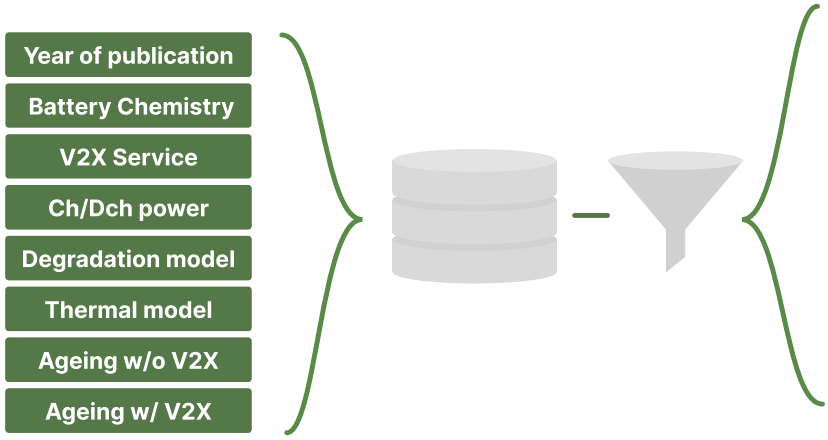

HIGHLIGHTS

- V2X raises degradation by 0.87% on average (95% CI: 0.35–1.4%).
- Adding degradation to the V2X optimisation limits the added degradation to 0.9%.
- Nearly all studies use semi-empirical models, giving a one-sided view of the problem.
- High contradiction between degradation results in V2X studies.

ARTICLE INFO

Keywords:
Vehicle-to-Everything (V2X)
Vehicle-to-Grid (V2G)
Ancillary services
Lithium-ion battery
Battery degradation

ABSTRACT

Vehicle-to-Everything (V2X) is a promising solution to support the energy transition, but concerns about battery degradation and capacity loss remain a major barrier for electric vehicle (EV) users. A clear understanding of degradation caused by V2X is essential to increase user confidence and encourage participation in V2X services. Many V2X studies have researched battery degradation, but the results vary widely between articles, making it hard to draw conclusions. Existing review articles mention the different outcomes but do not discuss the contradictions. In this article, a large set of V2X degradation studies is compared using a quantitative analysis. The yearly added degradation due to V2X is extracted from 37 V2X degradation papers, resulting in a set of 97 data points. The dataset is analysed to compare degradation in different situations and highlight contradictions in similar situations. Results show that the average yearly added degradation is 0.87% (95% CI: 0.35–1.4%). When degradation is explicitly considered in V2X service optimisation, the added degradation is limited to just 0.9% per year. Moreover, under specific conditions, V2X can even help reduce overall battery

* Corresponding author.
E-mail addresses: K.S.J.Linders@tudelft.nl (K. Linders), G.R.ChandraMouli@tudelft.nl (G.R. Chandra Mouli).

https://doi.org/10.1016/j.jpowsour.2025.238482
Received 19 June 2025; Received in revised form 12 September 2025; Accepted 24 September 2025
Available online 3 October 2025

degradation by reducing calendar ageing. Temperature and SoC are especially important in assessing the benefit of V2X on calendar ageing, but these factors are most often overlooked. This review has highlighted common shortcomings in V2X degradation literature that affect the assessment of the impact of degradation. The results can be used to clear up misconceptions about degradation in V2X and to guide future research directions.

Abbreviations

EV	Electric Vehicle
V0X	Standard Charging
V1X	Smart Charging
V2X	Vehicle to Everything
V2G	Vehicle to Grid
V2B	Vehicle to Building
V2H	Vehicle to Home
V2L	Vehicle to Load
FCR	Frequency Containment Reserve
FFR	Fast Frequency Response
aFRR	automatic Frequency Restoration Reserve
mFRR	manual Frequency Restoration Reserve
LS	Load Shifting
LS-C	Load Shifting with Cost optimisation
LS-G	Load Shifting with Grid optimisation
LS-B	Load Shifting with Battery optimisation
LS-N	Load Shifting without optimisation
PS	Peak Shaving
EA	Energy Arbitrage
RES	Renewable Energy Sources
NMC	Nickel Manganese Cobalt
LFP	Lithium Iron Phosphate
NCA	Nickel Cobalt Aluminium
DoD	Depth of Discharge
SoC	State of Charge
mSoC	middle State of Charge
SoH	State of Health
EoL	End of Life
LLI	Loss of Lithium Inventory
LAM	Loss of Active Material
LAM_{PE}	Loss of Active Material on the positive electrode
LAM_{NE}	Loss of Active Material on the negative electrode
RI	Resistance Increase
LoE	Loss of Electrolyte
EFC	Equivalent Full Cycle
SEI	Solid Electrolyte Interphase
CEI	Cathode Electrolyte Interphase
TM	Transition Metal
SPM	Single Particle Model
DFN	Doyle Fuller Newmann
SPMe	Single Particle Model with electrolyte

1. Introduction

With the increasing introduction of Renewable Energy Sources (RES) like solar and wind, the intermittency of power supply is a challenge for the grid. Meanwhile, the energy needed for transportation and heating that used to be delivered by a network of gas pipes and oil trucks is now transferred to the grid by replacing petrol cars and gas heaters with electric vehicles and heat pumps. This causes a high demand on the grid while the intermittency of supply is increasing. One of the solutions to provide flexibility to the grid, increase grid stability, and reduce peak demand is storing energy in Electric Vehicle (EV) batteries by implementing V2X. With the concept of V2X, the battery energy is allowed to flow in two directions. This enables the EV to store energy and support the grid during peak loads. Since cars are parked 95% of the time on average [1], they provide a huge storage opportunity when the market share of electric vehicles increases. Although the benefits for the grid seem eminent, the added use of the EV battery has raised concern with EV users [2–5]. The added charging and discharging cycles of V2X can potentially reduce battery life significantly [6–12]. However, in some scenarios the degradation was shown to be neglectable [8,10,13–16] or sometimes even reversed [10, 17–20]. The outcomes of V2X degradation studies are scattered and often contradictory. [6] reports that lifetime is reduced to 1 year after applying V2G, while [18] reports an increase in lifetime for a similar service and LFP cell. In [15], the authors measure added degradation of 0.27% per year, while [7] measures 6.2% added degradation for the same service. In [18], the authors report that V2X cycling causes higher degradation on NCA cells than leaving the cell at high SoC, while [21] reports the opposite for the same cell chemistry. This review aims to clear up contradictions and provide a unified story for the impact of V2X on battery degradation.

1.1. V2X applications

V2X is an umbrella term that includes all forms of bidirectional charging of electric vehicles. V2X applications include, Vehicle to Grid (V2G), Vehicle to Home (V2H), Vehicle to Building (V2B), and Vehicle to Load (V2L). The simplest application is to feed appliances or loads directly from the electric vehicle, known as V2L.

- **Vehicle to Home (V2H)**
  The vehicle is directly connected to a house, e.g. to reduce the grid dependency of a household, increase energy yield from solar panels, or store energy to reduce the energy bill.
- **Vehicle to Building (V2B)**
  The vehicle is connected to the building energy system to trade energy depending on the building load, grid prices, or renewable energy supply. With V2B, many EVs can simultaneously connect to the same energy system.
- **Vehicle to Grid (V2G)**
  The EV is directly connected to the grid to contribute to a selection of services, including direct access to the wholesale energy and ancillary services markets. The EV can operate solo or in a large fleet through an aggregator.

In each application, the battery energy can be used to provide multiple V2X services.

1.2. V2X services

The benefit of V2X has many positive predictions [3,22–25]. In a 2023 study [23], it was predicted that the grid storage demand could be met by 2030 when implementing EV battery storage, highlighting the potential impact of V2X technology. V2X services can provide high economic benefits [25] to EV users, especially when the efficiency of the converter and the charging power are high. Furthermore, V2B services can provide great benefits to building owners by reducing energy service costs, providing backup power during outages, and reducing the carbon footprint of the building [24]. In [22], the authors successfully reduced the grid load by 5%–10% using peer-to-peer power

transactions. In each V2X application, a selection of services can be provided. In [26], Thompson and Perez give an excellent review of V2X services and their connection to the energy market. In this review, not all possible services will be covered. Relevant services will be explained in the next sections, where some services will be grouped for clarity. Depending on the service, grid support can be constant or event-based. An example of a V2X service that is solely event-based is Peak Shaving (PS); only when the peak demand exceeds a threshold, energy is delivered back to the grid to decrease the demand peak. The load and the power threshold determine the frequency of service. In the case of FCR, service events can be forced by only enabling V2X during a set time period. This method is used in [8,11], where the FCR is provided for a certain time of day/month. In some countries, FCR is divided into two services, FCR-N for normal operation and FCR-D for disturbances [27]. EVs with V2X capability are not limited to a single service and can increase revenue by stacking multiple services [26]. Examples include the combination of FCR with PS [13,28], or FCR with LS [9,29].

1.2.1. Renewable energy storage

One of the greatest potentials of V2X is to store intermittent renewable energy. The stored renewable energy can later be used when the demand is high and renewable energy is not available. This application will increase the renewable energy penetration rate and reduce the dependency on fossil fuels.

1.2.2. Load shifting (LS)

Load Shifting (LS) refers to all situations where energy usage from the grid is moved in time. In some cases, LS is also referred to as Time Shifting. Shifting the load in time can have multiple objectives.

LS-C	Load Shifting to minimise energy costs
LS-B	Load Shifting to optimise battery degradation
LS-G	Load Shifting to improve grid health
LS-N	Load Shifting, where no particular optimisation is used

Firstly, LS could be used to minimise total energy costs, which is also called bill management. LS-C depends on dynamic energy prices. Revenue can be generated by optimising the charging profile based on the hourly spot prices. Whether these prices are available to residents highly depends on the location. In [30], an overview of the availability of dynamic pricing is given for European countries. The EV can be charged when prices are low and discharged when prices are high, or when energy is needed. When load shifting is applied without a building load, the EV battery can be used for trading energy, also referred to as Energy Arbitrage (EA). EA can provide high benefits, but the total storage efficiency has a large influence on the profitability [31]. In the case of V2X, this efficiency is determined by the charger's and battery's charging efficiencies and by the storage efficiency of the battery. In this review, all forms of load shifting with cost optimisation are referred to as LS-C. Another objective for charge profile optimisation besides costs is battery degradation, here referred to as LS-B. This optimisation requires some form of degradation model in the objective function. Studies have shown that battery degradation can be improved significantly when the charging profile is optimised for battery degradation [10,13,17]; this will be discussed further in Section 1.3. With LS-G, the load profile is optimised to increase grid quality. Examples are minimising load variance [8,32], improving grid flexibility [33], or congestion management [22]. LS-C can also improve grid load variance by incentivising charging during high-demand periods [34]. With LS-G, the grid load is directly considered without considering costs. With the last version of LS, LS-N, no particular optimisation was used. Although this is not a realistic scenario in V2X applications, some studies consider charging profiles where the EV (dis)charges at predefined times, like in [10] or [18].

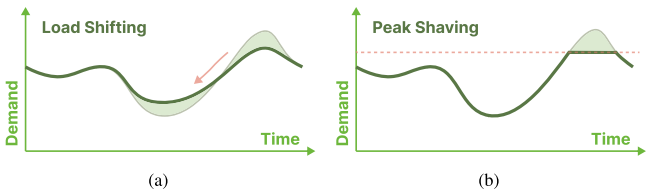

Fig. 1. Load profiles for (a) Load Shifting (LS), (b) Peak Shaving (PS). Light-coloured areas represent the original load profiles, and the dark lines represent the load profiles with the respective service.

1.2.3. Peak shaving (PS)

With PS, power is fed back when the demand exceeds a set limit P_{max}. The discharged power is used to keep the load at P_{max}. An example of PS is shown in Fig. 1(b).

$$P_{dsch} = P_{load} - P_{max} \quad \text{where} \quad P_{load} > P_{max} \tag{1}$$

Contrary to PS, Valley Filling (VF) fills the valleys in power demand by charging the battery when the demand is below a set limit P_{min}. PS has proven to lower the peak demand on the grid significantly. In [29], Visakh and Selvan measure a demand profile that is 17% flatter when implementing PS. In [34], PS reduces peak demand by 7.8% and load variance by 81.9%. PS can be especially valuable if the energy prices are influenced by peak usage, as can be the case in commercial applications [3,26,35].

1.2.4. Frequency services

A set of frequency services exists to keep the grid frequency stable and the load and generation balanced. In Fig. 2(a), the services are ordered by typical reaction time. In grids with limited inertia, EVs are well suited to support the frequency stability through Virtual Inertia or Fast Frequency Response (FFR) because of the fast response and instantaneous power delivery [36]. FFR provides fast restoration power in a response time typically below 2s [37]. FFR is a service that may assist primary frequency control in low-inertia grid systems [37]. In addition to FFR, the primary frequency service will adapt the output of the generating units to the grid. This service, called Frequency Containment Reserve (FCR), stabilises the grid frequency with a response time around 15 s. Participating balancing units will adjust their output power according to a droop curve as shown in Fig. 2(b). The power delivered by each generating unit is determined by the maximum power P_{max}, the maximum allowed frequency swing Δf, and the deadband frequency f_{DB}. These parameters will therefore influence the degradation when FCR is provided using V2G, as discussed in Section 4.4.1. When FFR and FCR have acted, the grid frequency will settle at a lower or higher value. The frequency is then restored to the nominal value by automatic Frequency Restoration Reserve (aFRR) and possibly manual Frequency Restoration Reserve (mFRR). While FFR and FCR are predominantly power-based services, aFRR and mFRR are energy-based services that provide energy for longer periods.

1.3. Literature review

As mentioned before, the outcomes of V2X degradation studies are scattered and often contradictory. Current review articles do not discuss the contradictions or compare a small number of sources. In a 2019 conference paper by Guo et al. [38], the authors give an overview of the degradation models used in V2X and provide a V2G impact analysis. The authors state that degradation with V2X charging depends on the battery chemistry and the provided service. The degradation results from the studies are not compared or shown in the review. In [39], the focus is on cyclic ageing measurements for different battery chemistries. The authors review several V2X studies that calculate cycle life and emphasise the importance of State of Charge (SoC) and Depth

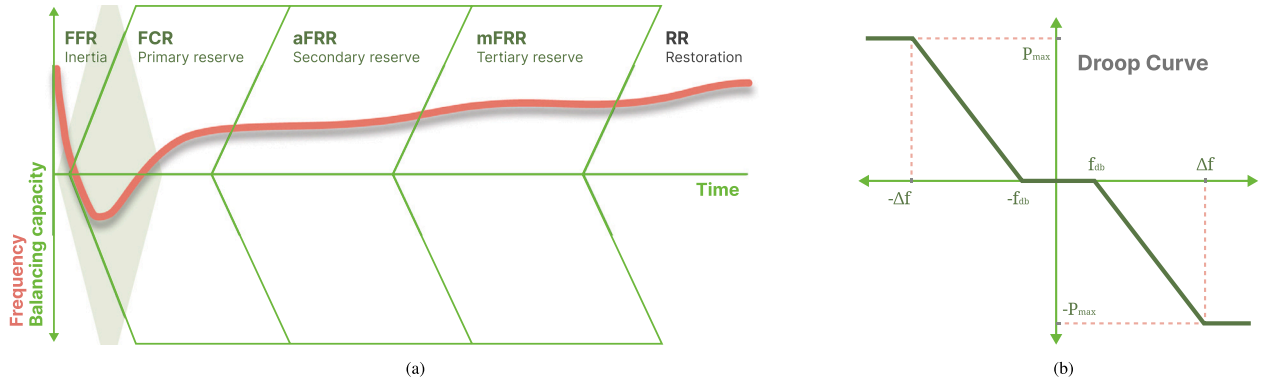

Fig. 2. (a) Frequency regulation services and (b) Droop curve for Frequency Containment Reserve (FCR) service.

of Discharge (DoD) during V2X. The review does not contain any V2X impact analysis or comparison between sources. [24] has a good review where the authors discuss the current state of smart buildings, including degradation due to V2X. The authors highlight that battery chemistries with high calendar ageing and low cyclic ageing can benefit most from V2G, and they indicate the lack of experimental studies. The authors indicate that there are not sufficient studies to refute or substantiate the concern of battery degradation and that the available results sometimes contradict. The article discusses some of the contradictions found in V2X results, but the article does not provide reasons for the contradictions, nor does it provide a quantitative comparison. In [40], the authors review V2X degradation studies focusing on battery models and optimisation strategies in V2B and V2G scenarios. The authors highlight the importance of modelling external influencing factors, like temperature, C-rate, SoC, and DoD. A detailed list of research gaps is given, but there is no impact analysis of V2X on battery degradation. In [4], the authors review the economic consequences of battery degradation when applying V2X. The authors give an overview of degradation mechanisms and review several V2X studies. The review article does not discuss the contradictions in V2X degradation results nor does it compare the quantitative results of the articles.

1.4. Research gaps and contributions

The reviews above give great insights into the considerations when applying V2X, but none of them quantitatively compare the amount of degradation due to V2X in the current literature. When users or manufacturers consider using V2X, knowing the expected added degradation is essential. Furthermore, contradictions in V2X degradation studies still remain unresolved. A quantitative analysis of battery degradation in V2X applications has not been seen in the current literature. This article reviews battery degradation with a clear overview of degradation stress factors for multiple popular battery chemistries. Degradation for different V2X services, battery chemistries, and operational parameters is compared. The influence of thermal management, charging power and locality is analysed. All the degradation findings are linked to known degradation phenomena in battery research.

This review provides the following added insights:

1. An overview of battery degradation phenomena for different Lithium-Ion battery chemistries, including interactions between the phenomena that affect the degradation
2. A review of degradation stress factors that couple operational conditions to degradation phenomena. The section reviews the sensitivity of different battery anode and cathode chemistries to conditions like temperature, C-rate, Depth of Discharge, etc.
3. An empirical study of 37 V2X studies that consider battery degradation. The analysis couples the results to the degradation stress factors to address contradictions in the results and gives quantitative insights into the added degradation by V2X.
4. Insights into optimising battery degradation with V2X are given, and trends in battery technology are connected to V2X opportunities in the future.

1.5. Structure

Section 2 gives a detailed review of battery degradation phenomena for common EV battery chemistries. Then, the sensitivity on operational parameters, like temperature, C-rate, DoD, and SoC, is compared for all chemistries and the influences are linked to degradation phenomena in Section 3. In Section 4, the results from 37 V2X degradation studies are compared, and the degradation impact is assessed and connected to the known degradation phenomena from Sections 2 and 3.

2. Battery degradation

Lithium-ion batteries consist of a negative electrode, a separator, and a positive electrode. In this review, we refer to the negative and positive electrodes as the anode and cathode. Energy is stored by transporting lithium ions from the cathode to the anode. During charging, the Li ions are first deintercalated from the cathode material, usually a layered structure of Transition Metals (TM). Then, the Li-ions move through the electrolyte and the separator towards the anode. The electrolyte most often consists of salt molecules like $LiPF_6$ and a solvent. At the anode, the Li ions are intercalated into the anode material. The most common anode material is layered graphite. Both electrodes are bonded to a metallic current collector, providing a path for the electrons to flow. The cathode current collector is often made of aluminium, while the anode current collector is often made of copper [41]. When reactions that do not contribute to this charging/discharging process occur, they are termed degradation mechanisms or side reactions. These unwanted mechanisms can cause the battery to degrade by taking lithium, electrolyte, or electrode material. Interested readers are referred to [42–45] for more information on battery degradation.

2.1. Degradation effects

From left to right, Fig. 3 shows the cause and effect relations in battery degradation. Battery degradation can become apparent in two ways: capacity fade and power fade. Capacity fade can be caused by a decrease in active lithium or by the loss of active electrode material to store the lithium. Power fade is caused by an increase in the internal resistance of the cell. Both capacity and power fade can influence the total driving range of an electric vehicle. When the power fade increases, the battery will be less efficient and lose more energy to heat.

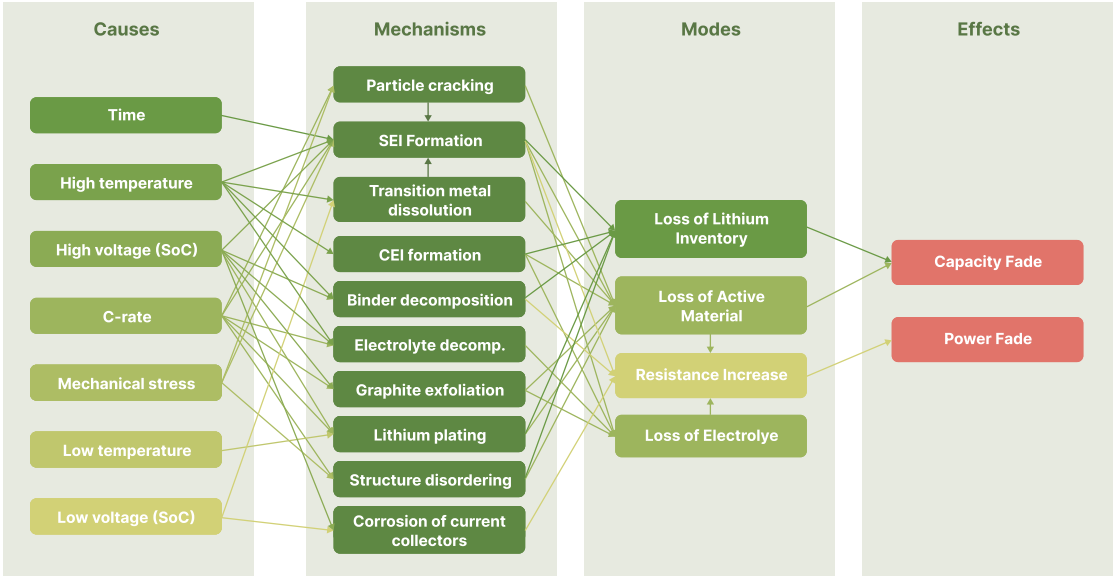

Fig. 3. Degradation causes, mechanisms, modes and effects presented graphically.
Source: This image is reproduced from [43,44,46].

2.2. Degradation modes

From left to right, Fig. 3 shows the cause and effect relations in battery degradation. The operating conditions in the left column influence the degradation mechanisms: the electrochemical side reactions in a Li-ion battery. The degradation mechanisms influence four degradation modes [43]:

- Loss of Lithium Inventory (LLI)
- Loss of Active Material (LAM)
- Resistance Increase (RI)
- Loss of Electrolyte (LoE)

When Lithium ions are consumed in side reactions, the lithium becomes trapped and cannot contribute to the storage reaction anymore. This is referred to as Loss of Lithium Inventory (LLI), which in turn causes a decrease in battery capacity. The second mode is Loss of Active Material (LAM), which can occur both at the anode side (LAM_{NE}) and the cathode side (LAM_{PE}). When active material at the anode or cathode is lost or damaged in a side reaction, the corresponding electrode can lose intercalation sites for the lithium, causing capacity fade. At the same time, the LAM can result in decreased surface area, resulting in a Resistance Increase (RI). At the same time, reactions that cause LoE increase cell resistance too, causing a decrease in the power capabilities of the cell. In some studies, RI is referred to as Conductivity Loss.

2.3. Degradation mechanisms

Battery degradation in Li-ion batteries is a complex process consisting of many mechanisms and interactions between these mechanisms. In Fig. 3, the reactions, the influences, and the internal interactions are connected graphically.

2.3.1. SEI layer formation

One of the biggest degradation mechanisms in a Li-ion battery is the formation of the Solid Electrolyte Interphase (SEI) layer. The SEI layer is a passivating layer that forms on the surface of the anode by reaction of Li^{0+} and the electrolyte [47]. The SEI layer is essential for the long-term use of the battery and exhibits electrolyte characteristics as it prevents the transport of electrons but conducts Li-ions [48,49]. At the same time, SEI layer formation is one of the biggest contributors to battery ageing as it consumes lithium inventory and increases battery resistance. SEI is considered a self-passivating reaction because it prevents electrons from reaching the outer layer of the anode particle and stops solvent molecules from percolating to the graphite layer [48]. This prevents the solvent molecules from reducing with electrons in the graphite layer. However, the SEI layer is not a perfect insulator, so Li-ions and electrons continue to react throughout the lifetime of the cell, causing the SEI layer to slowly grow over time [50]. The SEI layer takes about 10% of the initial Lithium Inventory in the forming stage, causing a steep decrease in the capacity [50]. This decrease in capacity happens at the factory during the first charge cycles under controlled conditions. After this first formation stage, the SEI layer grows steadily. The formation of SEI can be influenced by other mechanisms like Transition Metal (TM) dissolution and Particle cracking. When anode particles crack, an SEI layer forms on the newly exposed anode surface [51]. TM dissolution can accelerate the SEI formation significantly. When TM ions like Mn or Fe deposit on the anode, they can cause a chain reaction in the SEI layer, trapping additional Li ions. The effect of Li trapping causes an estimate of 10^2 Li+ ions to be trapped for every Mn^{2+} ion [48] The formation of the SEI layer is mainly influenced by high temperatures and high SoC. When temperatures are high, the chemical reactions that cause SEI formation accelerate [47]. When the SoC of the battery is high, the anode potential is low, causing the reactions at the anode surface to increase [52]. With the growth of the SEI layer over time, active lithium and electrolyte are consumed, leading to LLI and LoE [53]. Also, deposition of inorganic components from the cathode and electrolyte causes RI. [53]. Lastly, the SEI formation will cause Loss of Active Material on the negative electrode (LAM_{NE}), but the effect of LAM_{NE} is small compared to LLI and RI [48].

2.3.2. Particle cracking

Particle cracking is caused by the mechanical expansion and contraction of the electrode particle. When the battery is charged or discharged, the insertion of lithium in the electrode particle will cause uneven stress. Internally, the particle will be stretched due to the added lithium while the outside of the particle is compressed [51]. These uneven stresses cause cracks to form in the electrode particle. The growing cracks cause the surface of the particle to degrade and, in some cases, break off, resulting in LAM [54]. The formed cracks will, in turn, initiate new SEI layer formation on the exposed electrode surface. Particle cracking is mainly influenced by high charging rate and mechanical

stress [51,54,55]. The stability of the electrode material is an important factor in the amount of cracking. When the atomic structure of the electrode is rigid, the volumetric change during intercalation is low, like the LFP cathode [56]. Contrastingly, when the electrode material undergoes big volumetric changes during charging, the material is more prone to cracking, like with silicon anodes [57]

2.3.3. Lithium plating

In ideal conditions, all Li^+ ions are intercalated into the graphite structure at the anode. However, when the amount of Li^+ ions arriving at the surface becomes too large, Li starts plating on the outside in the form of Li metal [50]. When the amount of Li ions in the surface is very high, for instance, when graphite is fully-lithiated or when the lithium diffusion in the graphite is slower than the Li-ions are arriving at the surface, the potential at the electrode surface will drop to 0 V. This causes the Li-ions to prefer to deposit on the anode surface instead of intercalate into the graphite [50,58]. High charging rates and High SoC have a large influence on lithium plating. Because the diffusion rate of lithium inside the graphite is a function of temperature, a low temperature is also a main driver of lithium plating [58]. Lithium plating is one of the main limiting factors for fast charging of LiBs. One of the solutions being implemented today to reduce lithium plating is increasing the anode capacity relative to the cathode capacity [47].

When lithium is deposited on the surface of the anode, it tends to form in three different shapes: mossy, granular and dendrite [58]. At higher currents, the formation takes dendrite shapes. These dendrite formations can cause an internal short circuit by puncturing the separator. Hard shorts cause thermal runaway and destroy the cell. The created lithium metal deposits on the anode surface can be reversible or irreversible [58]. Irreversible lithium deposits cause both LLI and LAM_{NE}. LLI is caused when plated lithium detaches from the electrode, making it dead lithium [59]. This dead lithium cannot contribute to the charging reaction anymore and can react with the electrolyte, causing LoE [59]. The active material of the particle is influenced by Li plating due to continuous plating and stripping at the surface, causing local volume changes in the electrode structure. Lithium plating can accelerate the formation of the SEI layer [60]. The irreversible plated lithium can form a high-impedance layer called a secondary SEI layer [58].

2.3.4. Other mechanisms

Many other mechanisms exist in the battery. All can be seen in Fig. 3 and are explained in [42–45]. At high potentials, an SEI-like passivating layer grows on the cathodes too [47] referred to as Cathode Electrolyte Interphase (CEI). CEI contributes to LLI, Loss of Active Material on the positive electrode (LAM_{PE}), and LoE [46]. In nickel-containing cathodes like NMC or NCA, cation disorder can occur where Li and Ni ions switch places in the crystal lattice because Li^+ and Ni^{2+} have similar atomic radii [61]. The disordered nickel ions cause the diffusion channel to block, so other Li ions cannot pass the swapped nickel ion, resulting in LAM_{PE}. At the same time, the lithium ions will be locked into place, causing LLI. Especially batteries with high Nickel contents lead to a higher Li diffusion coefficient, lower cycling stability, and decreased overall electrode performance [62]. Transition metals from the cathode, like manganese, are soluble in the electrolyte. When this occurs, the ions can migrate through the separator and deposit on the anode side. This effect is mainly present in Mn-containing spinel cathodes, like LMO or LMNO, because manganese can be dissolved more easily [43]. When Mn^{2+} ions deposit on the anode SEI layer, they will catalyse the SEI formation, causing extra Li^+ ions to be trapped in the SEI layer [48]. In LFP cells, iron is also reported to dissolute and deposit on the anode [63]. For the anode current collector, copper is a commonly chosen material. Copper has a good electrochemical stability with potentials below 3 V vs Li+, making it a good choice for the anode current collector since the anode potential is often very low. However, when a battery is over-discharged, the potential at the anode will exceed the stability region of copper. At anode potentials around 3.7 V, the copper starts dissolving in the Electrolyte, causing pits in the copper surface. First, the copper is oxidised by water, causing the formation of Copper oxide. Then, the copper reacts with the HF molecules producing CuF_2. The dissolution of copper ions will cause Cu metal plating at the anode at low SoC, causing dendrites much like Li dendrites [41].

2.4. Battery chemistries

The most common anode material is layered graphite. Both electrodes are bonded to a metallic current collector, providing a path for the electrons to flow. The cathode current collector is often made of aluminium, while the anode current collector is often made of copper [41]. For the cathode, a large combination of materials can be chosen. Some materials have better power performance, higher energy density, or longer lifetime. In 2023, the Nickel Manganese Cobalt (NMC) cathode was leading the market for EV traction batteries with a 60% share, Lithium Iron Phosphate (LFP) following at 30%, and Nickel Cobalt Aluminium (NCA) reaching around 8% of global sales [64].

2.4.1. Nickel manganese cobalt (NMC)

The NMC battery has a layered oxide cathode structure with a mix of Nickel, Manganese, and Cobalt. The NMC battery is popular due to its high energy density (150–280 Wh/kg) and reasonably good cycle life (1000–4000 cycles). Before 2015, NMC batteries with an equal share of transition metals (NMC111/NMC333) were commonly used. But with rising cobalt prices, limited geographical availability of cobalt, and poor mining conditions in cobalt mines [65], manufacturers started reducing the amount of cobalt in the mix and increasing the amount of Nickel, creating NMC532, NMC622, NMC712, and NMC811. By increasing the total share of Nickel, the price is reduced, and the energy density can be increased because of the low mass and high conductivity of Nickel [66].

2.4.2. Lithium iron phosphate (LFP)

Next to NMC, LFP is the most popular cathode material. It has a lower specific capacity than NMC (90–180 Wh/kg) and a good cycle life (5000–7000 cycles). LFP consists of an olivine structure with a very strong covalent bond between the phosphorus and oxygen, preventing the oxygen from contributing to a thermal runaway, thus providing high thermal stability [67] and long cycle life [68]. LFP cells are a competitive choice due to their low price [69] because they do not contain rare earth transition metals like Cobalt or Nickel. Furthermore, the lack of Manganese or Nickel decreases degradation due to TM dissolution and cation disorder. Although the iron in the cathode can still dissolve, the resulting degradation is much lower [56].

2.4.3. Nickel cobalt aluminium (NCA)

The NCA cathode has a layered transition metal oxide similar to the NMC cathode. NCA offers high energy density (200–260 Wh/kg [70]) but a shorter lifetime (5̃00 cycles [70]) [38]. With NCA, manganese is replaced with aluminium, decreasing costs. A common mixture of NCA is $Li[N_{0.8}Co_{0.15}Mn_{0.05}]$ [71] where the amount of Cobalt is kept reasonably low. The NCA cell has lower thermal stability, making battery management more important [4].

2.4.4. NMC-LMO layered cathode

In some cases, like with early versions of the Nissan Leaf and the BMW i3, NMC is mixed with Lithium Manganese Oxide (LMO) to increase the power capabilities. LMO has an excellent diffusion rate due to the three-dimensional spinel structure [72], but mixing with LMO comes at the cost of faster degradation as LMO suffers from high surface dissolution of Manganese. With low SoC voltages outside of the stable region, the crystal structure is deformed by Jahn-Teller Distortion, causing Mn^{4+} to be reduced to Mn^{3+} [43,48]. Since Mn^{3+} is less stable, it tends to react by disproportionate into Mn^{2+} and Mn^{4+}, where especially Mn^{2+} is highly soluble in the electrolyte, causing accelerated growth of the SEI layer by lithium trapping.

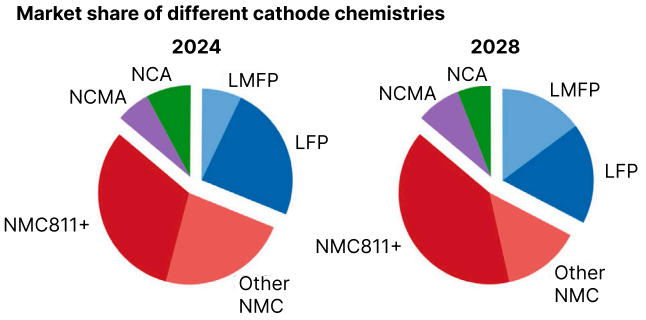

Fig. 4. Global outlook on the market share of battery chemistries for 2024 and 2028, based on information from [73].

2.5. Future trends

When looking at battery chemistries in the near future, three trends can be observed. The first is the expected growth in high-nickel NMC cathodes. In a global outlook from 2023, shown in Fig. 4 [73], the high nickel NMC811 chemistry is expected to dominate the market in 2028. Secondly, the market share of LFP is expected to decrease, making room for the new LMFP chemistry. The last observation is the increasing trend of NCMA. In another outlook from McKinsey 2023 [74], the authors anticipate the increase of LMFP and LMNO cathodes.

These forms of Li-ion improvements are sometimes called first-generation improvements since they are near-future improvements. There are many other promising solutions that are expected to become available soon. Two examples are the solid-state battery, based on a solid electrolyte instead of a liquid or gel, and the Sodium-ion battery, where the charge carrier is changed from Lithium to cheaper Sodium. For more information please visit the the battery roadmap.

2.5.1. High nickel NMC

A large trend in NMC cathode is to increase the amount of Nickel in the mix. Nickel has a positive influence on the energy density because the presence of Ni^{4+} ions increases the lithium insertion into the cathode [66]. Contrary to the increased capacity, the cathode suffers from higher degradation due to stronger reactions with the electrolyte [75] and increased cation disorder [76]. Furthermore, at high SoC the degradation is increased due to oxygen release and volume collapse in the cathode [77]. NMC811 shows 5–10 times more RI at a voltage of 4.20 V compared to 4.06 V, much higher than NMC532 and NMC640 cathodes, which have up to 2 times the resistance at 4.30 V compared to 4.10 V [77].

2.5.2. Silicon anode

In a graphite anode, six graphite atoms are needed to store a single lithium atom, causing a low energy density. Silicon provides a solution for increased energy density. With silicon, four lithium atoms can be stored for each silicon atom. The capacity of silicon is up to ã4200 mAh/g, 11x higher than that of graphite [78]. The advantage of the large capacity comes with a downside. Pure silicon anodes suffer from large swelling during charging. The volumetric increase of silicon (400%) is one of the biggest hurdles holding back implementation [79]. Adding small amounts of silicon to a graphite anode can increase the anode capacity without the large swelling of pure silicon anodes. The added silicon increases side reactions like gassing, SEI dissolution, and LoE [80]. These effects reduce calendar life and result in RI. The increased swelling of silicon causes particle cracking and increased SEI formation. The degradation at 100% SoC seems to be better [81] than with normal graphite anodes [52]. In [71] too, the resistance increase is lower with increasing SoC.

2.5.3. LMFP

The LMFP cathode combines the high safety of the olivine LFP cathode with the high energy density of the $LiMnPO_4$ cathode. The LMFP cathode faces issues with low charge and discharge rates due to the low electronic transport and low ion diffusivity of the material [82]. In recent studies, those limitations have been improved by, e.g. moderate Fe^{2+} doping and decreasing the particle size [83].

2.5.4. NCMA

The NCMA battery is a hybrid between NMC and NCA cathodes, forming $Li[Ni_{0.89}Co_{0.05}Mn_{0.05}Al_{0.01}]O_2$. The cathode provides a high capacity (similar to NMC) and a better cycling life than NCA [84]. With NMC batteries, high nickel content will cause decreased cycle life. By adding aluminium to the mix, the nickel content can be increased even further, as with NCA batteries.

2.6. Degradation modelling

To model the degradation of battery cells, three common model types can be distinguished: physics-based models, Machine Learning (ML) models, and semi-empirical models.

Physics-based models use a set of differential equations to model the electrochemical processes in the electrolyte and electrodes. A physics-based model can vary in complexity and accuracy. Three of the most used physics-based models are the Doyle Fuller Newmann (DFN) model, the Single Particle Model (SPM) and the Single Particle Model with electrolyte (SPMe) [85,86]. The interested reader is redirected to an excellent review on physics-based models by Planella et al. [85].

ML models learn to predict behaviour based on previous data it has been trained on. Many variations of ML degradation models exist. Although ML models are rarely used in V2X degradation studies, they are the most researched models in battery degradation studies (71% in 2023 [87]). Both [86,87] give an excellent overview of available ML models for battery degradation estimation and forecasting.

The last category of degradation models is the semi-empirical model. A semi-empirical model is created by fitting a line over measured battery data. Exponential powers, polynomials, and linear functions are common examples [19,34,88]. The advantage of a semi-empirical model is that it is easy to implement, fast to compute, and requires less data than ML models, making it a popular model for V2X studies. Because V2X studies almost solely use semi-empirical models, the next sections will focus on the semi-empirical model.

3. Connecting degradation stress factors to V2X

In many sources, a distinction is made between calendar ageing and cyclic ageing effects. Calendar ageing refers to ageing when the battery is not being used. Degradation effects, like e.g. SEI layer formation [47] and TM dissolution [48], can take place even when the battery is not charged or discharged. Cyclic ageing contains all ageing mechanisms that occur or accelerate when the battery is charged or discharged. In real applications, calendar and cyclic ageing occur simultaneously, so both calendar and cyclic ageing stress factors need to be considered. It is also important to note that the experimental cycle ageing test results include the effect of calendar ageing for the duration of the tests unless it has been subtracted from the results, utilising the knowledge from separate calendar ageing tests. If this is not taken into account when creating a combined cyclic and calendar ageing model, the model will effectively estimate the calendar ageing twice [89]. In [63], Lewerenz et al. estimated that the share of calendar ageing was 10%–30% of the total ageing of the cycle-aged LFP cells. Moreover, in [90] Redondo-Iglesias et al. concluded that the two ageing modes are not additive, but cyclic and calendar ageing interact.

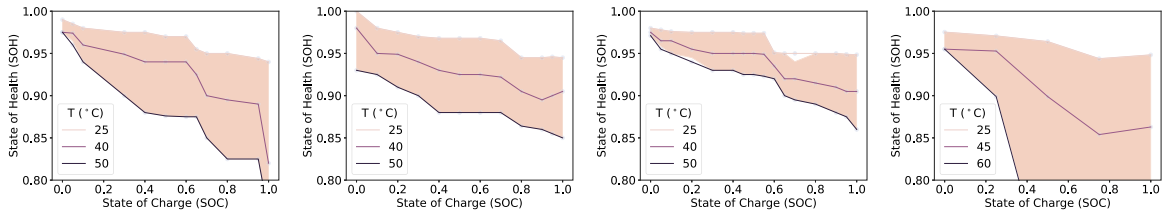

(a) NMC [52] (b) LFP [52] (c) NCA [52] (d) NMC-LMO [92]

Fig. 5. The effect of calendar ageing for three main cathode chemistries. Calendar ageing data from [52,92] were used to plot the SoH after 300 days of resting. The y-axis represents the SoH after 300 days for different resting SoCs (x-axis) and temperatures (line colour). The area between the highest and lowest temperatures is coloured to highlight the temperature dependency. For more details, please refer to [52,92].

3.1. Calendar ageing

Calendar ageing is influenced by the battery temperature and the SoC. When a battery is stored at high temperatures, side reactions like SEI formation are accelerated [47]. SEI layer formation is considered the largest contributor to calendar ageing [49,91]. Since the SEI layer is present at the anode, all cathode materials show similar dependency on the effects; high temperatures and high SoC increase degradation. The influence of temperature and SoC on calendar ageing does, however, differ per cathode material as shown in Fig. 5.

3.1.1. Temperature

It can be seen from Fig. 5 that the NMC-LMO cathode is most sensitive to storage temperature, followed by the NMC cathode. The figure shows the State of Health (SoH) after 300 days of calendar ageing at different SoCs for different storage temperatures. The dependency on temperature can be compared by the width of the pink area. A wide area indicates a high sensitivity to storage temperature. The influence of temperature on the calendar ageing of NMC cells has been studied in [89,93,94], and these studies found that higher storage temperatures accelerated cell ageing. With high temperatures the calendar ageing is accelerated due to increased SEI layer formation [47]. de Hoog et al. [89] linked the accelerated ageing in high temperatures to secondary side reactions such as corrosion at the negative electrode, and to increased LLI. The NCA cathode shows the lowest dependency on storage temperature. In [71], the capacity fade of NCA cells during calendar ageing was found to increase with temperature, and LLI was found to be the dominating degradation mode, indicating the effect of SEI formation. Calendar ageing results for LFP cells presented in [95–97] are consistent: high temperature accelerates the calendar ageing of LFP cells. Naumann et al. [95] conclude that the accelerated capacity loss and resistance increase are mainly due to the SEI growth on the graphite anode, which leads predominantly to LLI, and only a minor contribution is from LAM.

3.1.2. State of charge

As can be seen from Fig. 5, NMC and NMC-LMO batteries are most sensitive to the resting SoC. The sensitivity to SoC is visible by the steepness of the curve. The NCA cell is less sensitive to the SoC level and is more comparable to that of the LFP cell [98]. The calendar ageing of NMC batteries has been found to be faster the higher the SoC they are stored at [89,93,94,98]. Especially, long-term storage at 80% SoC or above seems detrimental for NMC cells. This has been suggested to be due to disequilibrium on the electrode/electrolyte interface, which contributes to side-reactions [89]. Also, with NCA cells, a higher storage SoC accelerates the capacity fade, with LLI identified as the key degradation mechanism [71].

Generally, the calendar ageing of LFP cells is faster with higher SoC [52,63,95,96]. However, Lewerenz et al. observed that the influence of SoC on LFP cell ageing is quite low compared to the influence of temperature [63]. In [95] Naumann et al. observed that in general, the capacity fade of LFP cells is stronger at high storage SoC, except that between 37.5–62.5% SoC they observed no difference in the rate of capacity fade, which is in line with the findings in [52]. In [97], the authors measure a shift in SoC dependency during calendar ageing of LFP cells when the capacity fade exceeds 20%. When the capacity fade is below 20%, a higher SoC results in higher degradation, but with a capacity fade above 20%, degradation is faster at mid-SoC levels. The effect on internal resistance remained similar.

3.1.3. Modelling

In semi-empirical models, calendar ageing and cyclic ageing are often modelled separately. Since calendar ageing is mainly influenced by SEI layer formation, many models focus on this mechanism. The SEI layer has been shown to grow with the square root of time [99]. [42,100] give a good review of calendar ageing models. The time dependency is often modelled as t^z where z is around 0.5 [19,46,88,101,102]. In semi-empirical models, the effect of temperature is modelled using the Arrhenius equation as [88]

$$Q_{loss\%} = Ae^{\frac{-E_a}{RT}}t^{0.5} \tag{2}$$

Where $Q_{loss\%}$ is the rate of capacity loss, A is a pre-exponential factor, T is the absolute temperature, E_a is the activation energy, and R is the Boltzmann gas constant. The two stress models are then combined by multiplying as shown in Eq. (2) [101]. The model from Eq. (2) can be expanded to include the SoC. The SoC dependency is often included in the exponential, the pre-exponential factor A, or both. In [103], the authors use a dependency on Voltage instead of SoC and include the voltage dependency in the pre-exponential factor $A(SoC)$ as a linear function. As shown in Fig. 5, the SoC dependency is not linear. In [104,105], and [106] the pre-exponential factor A was modelled with an e-power. This shape resembles the SoC dependency more closely and is similar to adding a factor to the exponential term. In [107], the authors updated the degradation model from [101] to include SoC dependency in the pre-exponential factor A, similar to the method of [104]. A piecewise linear function $A(SoC)$ is defined for different SoC values, based on the findings of [52].

$$A(SoC) = \begin{cases} -1.04 \cdot SoC^2 + 89.72 \cdot SoC + 1224.6 & SoC \leq 0.5 \\ 10.35 \cdot SoC^2 - 1083.6 \cdot SoC + 31447 & 0.5 < SoC < 0.7 \\ 2.64 \cdot Soc^2 - 409.55 \cdot SoC + 22035 & 0.7 \leq SoC \end{cases} \tag{3}$$

Lastly, the dependency on SoC can be included in the pre-exponential factor $A(SoC)$, activation energy $E_a(SoC)$ and time factor $z(SoC)$ as done by [18].

$$Q_{loss\%}(SOC, T, t) = A(SoC) \cdot e^{-\frac{E_A(SoC)}{RT}} t^{z_{cal}(SoC)} \tag{4}$$

The functions for A, E_a, and z_{cal} are determined by fitting measured data.

3.1.4. V2X context

Calendar ageing has a large effect on the degradation of the EV since cars are stationary for 95% of the time [1]. Lowering the resting SoC with V2X can increase the battery lifetime, but a trade-off should be

made between the reduction in calendar ageing and the added cyclic ageing. Leaving the battery at high SoC is not recommended. Since calendar ageing increases with high temperatures, it is best to enable thermal management at warm ambient temperatures. The effect of temperature is more pronounced at high SoC for NMC, NCA, and NMC-LMO, as can be seen in Fig. 5. Lowering the SoC through V2X might have a bigger benefit in warm weather conditions, except for LFP cells.

3.2. Cyclic ageing

As mentioned before, the ageing of a Li-ion cell is highly dependent on the battery chemistry. Batteries with an NMC or NCA cathode and graphite anode are most sensitive to DoD [108]. In contrast, batteries with LFP cathodes are insensitive to DoD but are most sensitive to discharge current due to the low diffusivity in the cathode [109]. In [110], LFP batteries were found to be most sensitive to temperature, followed by DoD, and least sensitive to middle State of Charge (mSoC). The mSoC is the centre SoC of the (dis)charge cycle. In [71], it was observed with NCA cells that DoD has a higher influence than temperature, charge rate and discharge rate, and the influence of the discharge rate depends on the SOC window.

Degradation reactions like Lithium plating [58], particle cracking [51], cation disorder [62], and graphite exfoliation [111] are all accelerated during cycling. Lithium plating, especially, can result in a high capacity loss at low temperatures, high C-rates, and high SoC [58].

Modelling. In many studies [88,101,103,104], the energy throughput is used to model the battery age. In these models, the energy throughput has a similar limiting function as time had with calendar ageing. In [88], the cyclic ageing is modelled as

$$Q_{loss\%} = Ae^{\frac{-E_a}{RT}}(Ah)^z \tag{5}$$

In many studies, the factor z is between 0.5 and 1 [46]. In the case of [88] $z = 0.5$, whereas in the case of [101], $z = 1$, making it a linear dependency on the energy throughput. In some cases, the energy throughput is included in the form of cycles as in [112].

$$C_{cyc} = a \cdot e^{b \cdot SoC} \cdot DoD^c \cdot N_{cyc}^d \tag{6}$$

Interestingly the Stroe et al. model the resistance increase linearly as

$$R_{cyc} = e \cdot DoD^f \cdot N_{cyc} \tag{7}$$

Some sources simplify the model to only depend on the number of full cycles [28]

$$C_{cyc} = \frac{\lambda_{cell}}{2 \cdot K_n \cdot DoD_{max}} |DoD(t)| \tag{8}$$

Where C_{cyc} is the cost of cycling, λ_{cell} is the price per Wh of the cell, K_n is the maximum number of cycles, DoD_{max} is the maximum Depth of Discharge of the cell, and $DoD(t)$ is the DoD during cycle t. This model can give a rough estimation of the degradation, but neglects all stress factors involved in ageing.

3.2.1. Temperature

NMC. The cycle life of NMC cells is reduced at both low and high temperatures. When charging at lower temperatures, Li plating occurs at the anode side [58,113], especially at high C-rates. In [114], decreasing cycling temperature from 25 °C to 10 °C and 0 °C was observed to decrease the cycle life of NMC811 cells. This is mainly due to the decreased transport and reaction characteristics at low temperatures [114].

Many studies report accelerated NMC cell ageing at temperatures above 25 °C [108,113,115,116]. It must, however, be noted that the effect of calendar ageing is often included in the results. At high temperatures, ageing is accelerated due to increased side reactions [114] like SEI layer growth and TM dissolution [113].

In [114], cycling the cells at 40 °C increased the cycle life when charged with 1C but decreased the cycle life when cycled with 0.5C [114]. Schindler et al. explained the improved cycle life at 1C with the improved transport and reaction characteristics at 40 °C. The decrease in cycle life at 0.5C can be explained by the longer cycle time and calendar ageing effects as well as the lower cyclic ageing effects at 0.5C.

LFP. In the same way as with NMC and NCA batteries, cycling at low or high temperatures reduces the cycle life of LFP cells while the optimum temperature is close to 25 °C [96,117]. In [96], LFP cells were cycled in 7 different temperatures from 0 °C to 55 °C and the lowest capacity loss was observed at 25 °C. In [110], cycling LFP cells at 50 °C was observed to accelerate ageing compared to cycling at 35 or 42 °C. In [118], the authors attribute this partially to dissolution and deposition of Fe on the anode.

NCA. The effect of ambient temperature on NCA cell cycle ageing is similar: at higher temperatures, the ageing rate is bigger, but on the other hand, at very low temperatures, Li plating might appear and accelerate the ageing [119]. Cycling NCA cells at sub-zero temperatures causes a rapid drop in capacity, mainly due to Li plating at the graphite anode [120]. In [71] Wildfeuer et al. observed that increasing cycling temperature above 20 °C accelerated the capacity fade and RI of NCA cells, especially when the temperature was raised from 35 °C to 50 °C.

Modelling. Temperature in cyclic ageing can be added in multiple ways. In [88], the authors propose a cyclic model based on the Arrhenius equation as shown in Eq. (5). An Arrhenius dependency can provide a reasonable estimate of temperature dependency at higher temperatures. Still, since cyclic ageing also depends on Lithium plating, particle cracking, and other side reactions, the estimation breaks down at lower temperatures and higher C-rates. The authors recognise that the model does not hold at temperatures below 0 °C and higher C-rates. A corrected model for LFP cells was proposed in [18,88] for high C-rates, where the pre-exponential factor A and the activation energy E_a depend on the current I_{rate}.

$$Q_{loss\%} = A(I_{rate})e^{\frac{-E_{a0}+\alpha|I_{rate}|}{RT}}(Ah)^z \tag{9}$$

In 2014, the authors defined a similar model for an NMC-LMO cathode as shown in Eq. (10) [101]. This model does not use the Arrhenius dependency but still models an exponential dependency on temperature and C-rate.

$$Q_{loss,\%} = (aT^2 + bT + c)e^{(dT+e)I_{rate}}Ah_{throughput} \tag{10}$$

A review of semi-empirical models by Vermeer et al. [46] reveals that very few models consider low temperatures below 10 °C. This limits the capability of semi-empirical models to estimate degradation in low-temperature conditions, as the extrapolation of the equations will not catch the extra dynamics of phenomena like lithium plating.

V2X context. At low temperatures, cyclic ageing increases, and calendar ageing decreases. The cyclic ageing will likely be higher when performing V2X at low ambient temperatures. Contrastingly, at high ambient temperatures, the cyclic ageing of V2X will have a lower impact, and the impact of calendar ageing at high SoC will be larger. This would suggest that V2X is more beneficial at high ambient temperatures. In some cases, thermal management can be enabled during V2X charging to decrease cyclic ageing.

3.2.2. State of charge

NMC. The cycle life of NMC cells has been observed to decrease with high mSoC [89,121–123], in addition to which some studies have observed accelerated ageing also with low mSoC [122,123]. de Hoog et al. cycle aged NMC cells with multiple mSoC and concluded that faster cell degradation occurs at elevated mSoC [89]. Similarly, Krupp et al. observed accelerated capacity loss with 90% and 70% mSoC compared to 50% mSoC [121]. In [123], NMC cells were cycled with

10% DoD around different mSoC, and high and low SoC ranges showed the fastest degradation, while the lowest degradation was observed around 50% SoC. In [122] Gao et al. cycled NMC cells with 20% DoD at five SoC ranges and observed that cycling under 0%–20% SoC caused the least capacity loss but the most impedance increase, whereas cycling under 80%–100% SoC caused the most capacity loss with LLI as the dominant factor. In [108] Olmos et al. deduce from the data found in the literature that the optimal mid-SoC is around 50%, while lower and higher mSOC accelerate the ageing of NMC cells.

LFP. For LFP chemistry, there are fewer studies on the effect of mSoC, and therefore, there is more uncertainty. In [124], Jiang et al. observed that LFP cells cycled between 75%–100% SoC exhibited the fastest capacity degradation, followed by cells cycled between 0%–25%. In contrast, cells cycled between 25%–50% SoC and 50%–75% SoC showed superior cycling performance. On the other hand, Guo et al. cycled LFP cells with 35% DoD with three mSoCs and observed that 27.5% mid-SoC resulted in the lowest capacity fade while cells with 50% and 72.5% mSoC aged equally [110]. Also Olmos et al. concluded that there is not enough data for analysing the effect of mSoC properly [108].

NCA. The cycle life of NCA cells has been found to decrease when they are cycled at high mSoC [71,125]. Benavente-Araoz et al. observed that cycling NCA cells with middle and low mSoC (35%–65% SoC and 20%–50% SoC, respectively) reduced the capacity loss rate compared to high mSoC (65%–95% SoC) [125]. In [71], the ageing of NCA cells accelerated when cycled at high mSoC, most likely due to particle cracking in the cathode.

Modelling. In [112], the authors define a model as shown in Eq. (6) that depends on the middle SoC and the DoD. The authors model the resistance increase without a SoC dependency. In an article by Schmalstieg et al. [103], the authors use a quadratic function that includes SoC by including average Voltage.

$$Q_{loss,\%} = (a \cdot (V_{avg} - b)^2 + c + e \cdot DoD) \cdot Ah^{0.5} \tag{11}$$

Here, V_{avg} is the average Voltage during the cycle.

V2X context. High SoC accelerates Li-ion battery calendar ageing, while, depending on the Li-ion chemistry, high mid-SoC and low mid-SoC during cycling have been found to accelerate ageing. Therefore, SoC should not be considered only as a calendar ageing stress factor; the effect of cycling at low SoC should also be considered.

3.2.3. Charge and discharge current

Charging and discharging rates are connected to a large number of degradation mechanisms. High charging currents increase the chance of Lithium plating [58], graphite exfoliation [111], particle cracking [51], and electrolyte decomposition [111]. High discharging currents increase particle cracking and structural disordering at the cathode side [126].

The impact of charge and discharge current is highly dependent on the temperature [114]. At temperatures below 25 °C, effects like lithium plating and particle cracking are accelerated [51]. At temperatures above 25 °C, the transport and charge reactions are improved [114]. In some cases, higher C-rate causes cell heating that accelerates calendar ageing effects [127]. In [127], Barcellona and Piegari concluded that not C-rate but temperature is the main driver in LCO battery degradation for C-rates up to 5C and 95% SoC.

NMC. In [114], the cycle life decreased from 0.5C to 1C except at an ambient temperature of 40 °C. Schindler et al. explained the improved cycle life at 1C with the improved transport and reaction characteristics at 40 °C. The decrease in cycle life at 0.5C can be explained by the longer cycle time and calendar ageing effects as well as the lower cyclic ageing effects at 0.5C.

High discharge current accelerates the ageing of NMC batteries [108]. In [128], high charge currents were found to have a more significant influence on the capacity degradation of NMC cells than high discharge currents. In [129], a higher charge current was found to accelerate the ageing of NMC811 cells, and the predominant ageing mode was identified to be LLI.

LFP. In general, both higher charge and discharge current accelerate LFP battery ageing. In [130], LFP cells were cycled with different discharge rates from 0.5C to 5C, and it was observed that the capacity fade rate increased as a function of discharge rate. In [63], high-power LFP cells were cycle aged with 1C, 2C, 4C, and 8C, and the decrease in capacity was faster the higher the C-rate, except with 4C, which showed capacity fade comparable to 1C. Lewerenz et al. linked this to increased core temperature of the cell that could lead to more homogeneous and less severe ageing, whereas with 8C the temperature would reach a crucial limit and lead to different ageing effects [63]. Schimpe et al. cycle aged LFP cells with 0.25C, 0.5C, and 1C at 10 °C and 55 °C, and observed that at low temperature pure cycle capacity loss increases with C-rate whereas at high temperature the capacity loss is similar for all C-rates tested [96]. They attributed the correlation of ageing with C-rate at low temperatures to low-temperature ageing mechanisms such as capacity losses due to transport limitations, possibly lithium plating, that correlate with high charge current rate [96]. In [131] Naumann et al. observed that higher charge and discharge rates lead to faster ageing when the calendar ageing is subtracted, although they noted that the difference was small.

NCA. In [132,133], a positive effect on higher discharging current is reported for NCA/Gr batteries. In [132], Preger et al. measure the degradation of commercial NCA/Gr cells at 0.5C, 1.5C, and 2C discharging currents at 15 °C, 25 °C, and 35 °C. In [133], Cui et al. measure the degradation at 1.5C and 2C and 25 °C. Both authors conclude that low discharging currents increase battery degradation. A concise explanation is not given in either study. [133] blame the measured increased resistance at lower C-rates, but do not give a reason for the added resistance. [132] considers that the higher C-rate increases cell temperature, but the authors do not see a large temperature dependence across the measurements. In [71], the authors measure a decrease in lithium plating with NCA cells cycled at higher C-rates, but this is most likely due to internal cell heating. In a V2X study with NCA/Gr cells by Uddin et al. [17], the authors also measure an increased resistance with lower C-rates. In [119] Su et al. found that both higher charge and discharge current accelerated NCA cell ageing, although the effect was smaller for the discharge current. Since other sources [134] also report a negative dependency on discharge current, the effect of discharge rate on NCA batteries is considered indecisive.

Modelling. In semi-empirical models, C-rate is often included in the exponential factor, as shown in Eq. (9) and (10). In [19], the stress factor from C-rate is linearly interpolated from data between 0.3C and 2C. The combined influence of temperature and C-rate is not considered. The combined influence of temperature and C-rate is vital [101]. In [101], the capacity loss increases with increasing C-rate at 10 °C, while the capacity loss shows a parabolic shape at higher temperatures. In [46], the authors present an overview of semi-empirical models that show that very few models account for temperatures below 10 °C. This makes sense for EVs with thermal management, but should be considered when thermal management is not included.

V2X context. Higher C-rates can accelerate ageing due to V2X. The impact of cell-heating with higher C-rates should be considered when modelling degradation. Since the impact of C-rate is very dependent on the cell temperature, the two factors should be modelled together.

3.2.4. Depth of discharge

NMC. The dependency on DoD is highly dependent on the battery chemistry. The NMC battery is most sensitive to DoD [108], more than, e.g. LFP or NCA cathodes. In [123], the cycle life of NMC cells is significantly higher with shallow DoD compared to higher DoD. In more

recent studies, the finding is the same: cycling NMC cells with lower DoD results in higher cycle life [89,93,94,121]. Frambach et al. cycled large-scale NMC cells with 1C around 50% mid-SoC with 60%, 75% and 90% DoD, and observed significantly accelerated capacity fade with 90% DoD compared to the lower DoDs [94]. In [121], Krupp et al. tested NMC cells with six different DoD and observed that 5%, 10% and 20% DoD resulted in relatively low capacity loss, 40% DoD in moderate capacity loss, and 50% and 60% DoD in the highest capacity loss with almost equal rate.

LFP. For LFP batteries, the dependency on DoD is much lower compared to NMC batteries [68,88,108]. In [108], the lifetime is slightly better with higher DoD. In [118], the authors also conclude that high DoD reduces the degradation of LFP cells, but the authors test the cells up to approximately 800 cycles. On the other hand, Guo et al. [110] observed significantly accelerated capacity fade with 60% DoD compared to 10% and 35% DoD. In [131], Naumann et al. noticed increased degradation when using low DoD, but the effect reverses after 2000 cycles, resulting in an overall increase of degradation with higher DoD over the full lifetime. In conclusion, the lifetime of LFP cells seems to increase with higher DoD, but the effect is inconclusive after 2000 cycles.

NCA. The NCA cathode is also sensitive to cycling with high DoD [71,135]. Especially cycling with 100% DoD was found to rapidly accelerate NCA cell ageing, mostly driven by Loss of Lithium Inventory (LLI) and Loss of Active Material on the negative electrode (LAM_{NE}) [71]. In [135], significantly lower capacity fade was observed for NCA cells cycled with 60% DoD (10%–70% SoC) compared to 100% DoD.

Modelling. DoD is included in almost all models in the form as seen above, but few studies include the real degradation dependency of DoD. In [15,136,137], the authors use a Wöhler curve to model the degradation, as shown in Eq. (12) [136]. The Wöhler curve is widely used in mechanics to model the fatigue of materials. The model neglects the influence of SoC, Temperature, or C-rate but does include a DoD dependency.

$$Q_{loss,\%}(DoD) = \frac{n_{DoD}}{C_{life} \cdot DoD^{-k}} \tag{12}$$

Where n_{DoD} is the number of cycles performed at a given DoD, C_{life} is the nominal cycle life of the battery, and k is the constant describing the ageing speed of a certain battery type. In [138], a similar approach is used, but now the cycle life C_{life} is adjusted based on the used DoD, resulting in

$$Q_{loss,\%}(DoD) = 0.2C_{bat}\frac{1}{C_{life}(DoD) \cdot DoD} \tag{13}$$

In [104], the authors noticed an inter-dependency between the DoD and the Ah-throughput. Therefore, they modelled the Ah throughput with a power law for two different DoD regions as

$$Q_{cycl} = \begin{cases} (\gamma_1 DoD^2 + \gamma_2 DoD + \gamma_3) \cdot Ah^{0.87} & 0.1 \leq DoD \leq 0.5 \\ (\alpha_3 \cdot \exp(\beta_3 \cdot DoD) + & \\ \quad \alpha_4 \cdot \exp(\beta_4 \cdot DoD)) \cdot Ah^{0.65} & else \end{cases} \tag{14}$$

V2X context. The DoD will be influenced by the provided V2X service. An energy-intensive service like EA will result in deeper discharge cycles than a service like FCR. The deeper cycles can result in more degradation for NCM and NCA cells. How the degradation is presented is important for the interpretation of the results. Some sources report the amount of degradation over the cycle count, some report the degradation over time, and others report the degradation over the cycle life or Equivalent Full Cycle (EFC). In an example study by Carmeli et al., the lifetime of NMC cells was reduced by implementing higher DoD V2X, but the total energy throughput doubled [139].

3.3. Chemistry comparison

The operational stress factors affect NMC, LFP, and NCA chemistries differently, leading to varying degradation behaviours. NMC cells show the strongest sensitivity to both high and low mSoC, as well as wide DoD windows. Studies report faster degradation at both low and high mSoC [122,123], with optimal ageing performance around 50% SoC [123]. DoD has a particularly strong effect on NMC cells; higher DoD significantly reduces cycle life [89,93,94,121].

In contrast, LFP cells are relatively robust against SoC variations. [110] observed minimal difference in capacity fade across different mSoCs, although some studies noted faster ageing at SoC extremes [124]. LFP's primary sensitivity lies in temperature and C-rate. Its low diffusivity makes it vulnerable to lithium plating and transport limitations at low temperatures and high charging rates [96]. [96] found significant capacity fade acceleration in LFP cells at both 0 °C and 55 °C, with optimal performance near 25 °C.

NCA cells exhibit strong degradation under high mSoC cycling, with faster capacity loss linked to cathode particle cracking and SEI growth [71,125]. However, studies also report unexpected benefits at higher C-rates, attributed to internal heating that reduces lithium plating [71,133]. Unlike NMC, NCA seems less sensitive to DoD.

These distinctions show that degradation-aware V2X control must consider chemistry-specific sensitivities. NMC systems require careful SoC and DoD management, LFP systems need better thermal and C-rate control, while NCA benefits from avoiding high SoC and low temperature/low C-rate cycling.

4. Impact of V2X on degradation

This section compares the outcomes of 37 V2X studies considering battery degradation. The amount of added degradation is extracted from V2X studies that reported the amount of degradation for EV charging with and without V2X. Some studies reported the degradation for multiple V2X services or cases, resulting in a dataset of 96 degradation measurements.

4.1. Method

The compilation of the dataset consists of two steps: article selection and data extraction. Articles are searched from Scopus and Web of Science using the following query:

(battery OR batteries) AND (degradation OR ageing OR ageing OR deterioration) AND (v2x OR v2g OR v2 h OR v2b OR v2c OR v2l OR v2v OR v2p)

All unique results (339) are filtered based on the title, giving a dataset of 53 degradation studies considering battery degradation in combination with V2X studies. Then, the resulting 53 results are included in the analysis if they contain numerical results for degradation with and without any V2X service. The selection results in 37 studies on the topic of V2X service and battery degradation that report degradation results. The degradation is reformatted to a yearly added degradation to compare the results from the studies, both in text and figures. In case the SoH after time t is reported, the yearly degradation is estimated linearly by

$$\Delta SoH_t^{V2X} = \frac{\delta_t^{V2X} - \delta_t^{V0X}}{t} \tag{15}$$

where δ_t is the degradation in % at time t in years.

$$\delta_t = SoH_0 - SoH_t \tag{16}$$

SoH_t is the reported SoH at time t in %.

Some studies only report the battery lifetime instead of SoH. In these cases, the yearly degradation is calculated by assuming a linear decrease until the reported End of Life (EoL) (usually 70%–80% SoH).

$$\delta_t = \frac{EoL}{t_{life}} \tag{17}$$

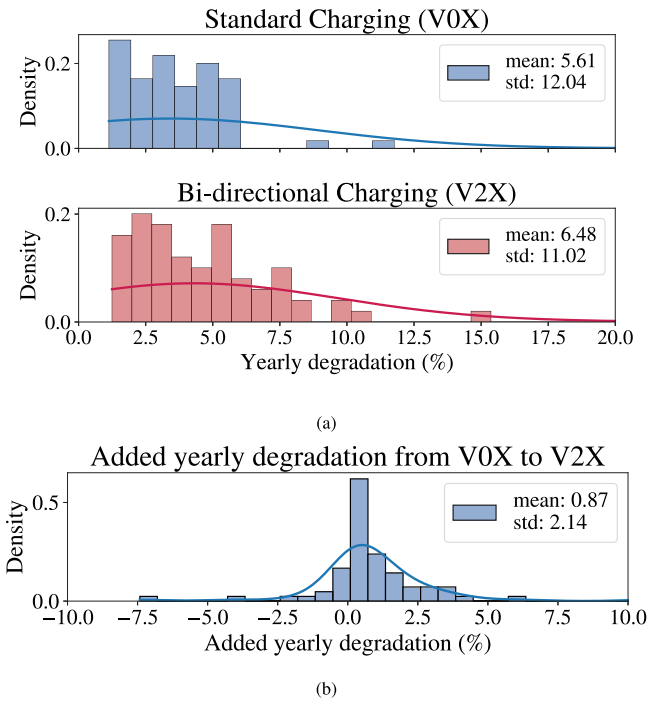

Fig. 6. Yearly degradation distribution based on 97 data points. The mean and standard deviation of the data sets are shown in the plots. (a) Shows the distribution of yearly degradation with and without V2X. (b) Shows the distribution of added yearly degradation when going from V0X to V2X.

Table 1
Summary of the statistical results from the degradation dataset in Fig. 6. The values are based on mean, standard deviation (Std), and the 95% confidence interval bounds (low and high).

	V0X	V2X	Added
Mean	5.45%	6.85%	0.87%
Std	12.04%	11.02%	2.14%
Low	2.65%	3.77%	0.35%
High	8.56%	9.19%	1.4%

Where EoL is the defined end of life and t_{life} is the reported lifetime from the study. The proposed method is admittedly oversimplified but sufficient for comparison purposes. Whenever a degradation percentage is given, we refer to the yearly degradation, unless specified otherwise.

Table 2 gives an overview of V2X degradation studies. The table shows the used cathode chemistry, V2X application and provided service, stress factors considered in the degradation model, if battery degradation was considered in the optimisation, the thermal model used, and the amount of added degradation in the study. In Fig. 6, the distribution of degradation results is shown. The figure is based on 97 data points from V2X degradation studies. In Fig. 6(a), the distribution for V0X and V2X degradation is shown. The average degradation with uncontrolled charging (V0X) is 5.61%. The average degradation with V2X is 6.48%.

4.2. Limitations

Because the dataset is relatively small, and because the methods and conditions vary widely from study to study, the results should be interpreted carefully. As can be seen from Fig. 6(a), the spread in degradation for both V0X and V2X is very wide. In Table 1, statistical data is shown to highlight the big spread in degradation results. The 95% confidence interval bounds are shown by the value low and high. Fig. 6(b) shows the added yearly degradation when going from V0X to V2X. The dataset has a confidence interval between 0.35% and 1.4% added yearly degradation. In Fig. 7, all the samples are shown for transparency and the confidence intervals are shown for all chemistries. As can be seen, the confidence for NMC and NMC-LMO are tight, while values for LFP and NCA are uncertain. This highlights the research gap for LFP and NCA chemistries. Data from RecurrentAuto concludes an average EV degradation between 1%–2% for EVs with uncontrolled charging [156]. The average degradation in Fig. 6(a) is considerably higher, even in the case of V0X. This indicates that the absolute degradation due to V0X and V2X may be lower.

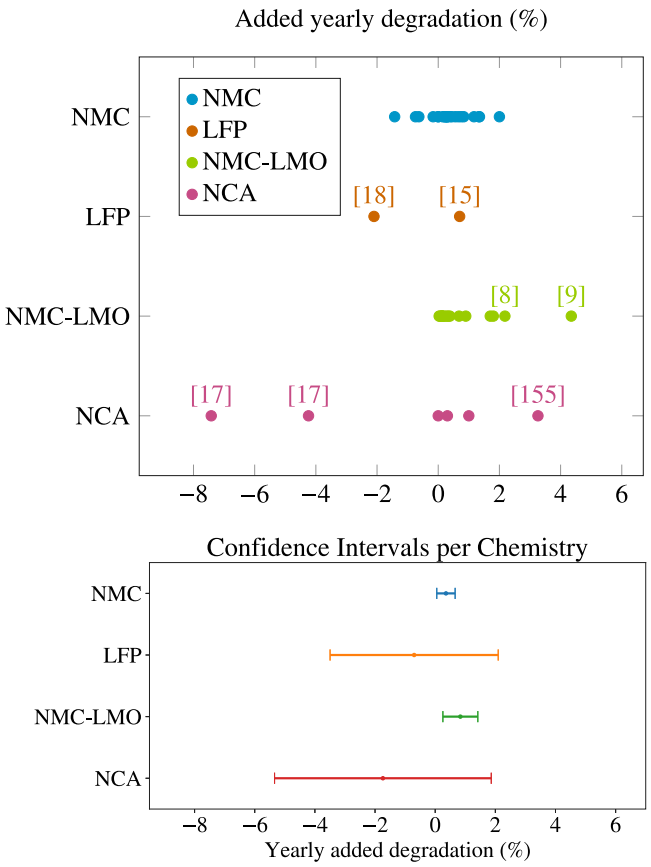

Fig. 7. Yearly added degradation as extracted from the articles. The top figure shows the data points with citations discussed in the text. The bottom figure shows the 95% confidence intervals of the data per chemistry.

In Fig. 8, the degradation of Bishop et al. [6]is indicated with an arrow. The degradation is a clear outlier with added degradation of 25% per year. For this reason, the study was not included in the numerical analysis. Section 4.4.3 discusses the study in more detail.

4.3. Battery chemistry

Fig. 7 shows the yearly added battery degradation for different cathode materials. It can be noticed that both LFP and NCA have relatively low average degradation compared to NMC and NMC-LMO cathodes. This aligns with the degradation described in Section 2. However, because there is little research available for these chemistries, the confidence interval is very large. For NCM and NMC-LMO, the confidence interval is tighter but always positive. In V2X studies, high DoD is linked to higher degradation when using NMC and NMC-LMO batteries [10,28,32]. [10] applies V2X cycling profiles to real NMC pouch cells and measures the degradation. In [32], the authors simulate the degradation using semi-empirical models for NMC and LFP cells. In [88], the authors derive a semi-empirical degradation model for LFP

Table 2
V2X studies considered in the degradation analysis. The battery cathode chemistry, modelled stress factors, provided service, optimisation, and thermal model are listed.

Study	Cathode	Connection			Calendar		Cyclic					Ageing Model	Service	Ageing in opt.	Thermal model
		V2G	V2H	V2B	T	SoC	T	SoC	DoD	C-rate	Ah				
2025															
[140]	NMC622		x		x	x	x	x	x	x	x	[140] (2025)	LS-N	no	Cell heating
2024															
[141]	NMC	x		x	x	x	x			x	x	[101] (2014)	FCR, LS-C	yes	RC model
[142]	NMC-LMO		x	x	x	x	x			x	x	[52,101]	LS-C, LS-B	yes	–
[143]	NMC		x		x	x	x	x	x	x	x	[143] (2024)	LS-N	no	–
2023															
[9]	NMC-LMO	x		x	x[a]	x[a]	x			x	x	[101] (2014)	FCR, LS-C	yes	RC model
[15]	LFP	x						x	x		x	[112] (2016)	FCR	no	–
2022															
[10]	NMC111		x	x	x	x	x	x	x	x	x	[10] (2022)	LS-N	no	Real cell
[139]	NMC	x			x	x	x	x		x	x	–	FCR	no	RC model
[144]	LFP			x						x		–	FCR, LS-C	yes	–
[145]	LFP	x							x		x	[104] (2015)	LS-C	yes	–
[29]	?	x							x	x		[146] (2012)	LS-C	yes	–
[147]	?	x							x	x	x	[148] (2012)	LS-G	yes	–
2021															
[19]	NMC811	x			x	x	x			x	x	–	LS-B	yes	–
[13]	NMC	x			x	x	x	x	x	x	x	[105] (2018)	FCR, PS	no	–
[14]	NMC	x			x	x	x		x	x		[2] (2020)	LS-N	no	Cell heating
[12]	NMC		x		x	x	x	x	x	x	x	[12] (2021)	LS-N	no	Real cell
[149]	NMC-LMO	x			x	x	x			x	x	[8,107] (2016)	FCR	no	Real vehicle
2020															
[28]	?	x	x	x					x	x		–	FCR, PS	yes	–
[42]	NMC-LMO		x		x[a]		x			x	x	[101] (2014)	FCR, LS-C	yes	–
[16]	NMC-LMO	x			x[a]	x[a]	x		x	x	x	[101] (2014)	FCR	no	Outside temp
[20]	NMC		x		x	x			x	x	x	[103] (2014)	LS-C	yes	–
[150]	NCA	x			x	x	x	x	x	x	x	[150] (2020)	FCR	no	Real cell
[7]	LMO	x			x	x	x	x	x		x	[105] (2018)	FCR	no	–
[151]	?		x				x	x		x		–	FFR, LS-C	yes	–
[152]	?	x								x	x	[153] (2011)	LS-C	yes	–
2019															
[137]	NMC			x					x	x		[138] (2016)	LS-C	no	no
2018															
[154]	LFP		x		x	x	x		x	x	x	[88,104] (2011)	–	–	–
2017															
[155]	NCA	x			x	x	x	x	x	x	x	[155] (2017)	LS-N	no	–
[17]	NCA	x		x	x	x	x	x	x	x	x	[17] (2017)	LS-B	yes	RC model
[11]	NMC	x					x		x	x		–	LS-N	no	Cell heating
2016															
[8]	NMC-LMO	x			x[a]	x[a]	x			x	x	[101] (2014)	FCR, PS, LSHP	no	Cell+solar heat.
[18]	LFP/NCA	x			x	x	x			x	x	[88] (2011)	LS-N	no	–
2015															
[32]	NMC/LFP	x			x	x				x	x	–	LS-B	yes	–
2013															
[6]	LFP	x					x			x	x	[88] (2011)	FFR	no	–
2010															
[68]	LFP		x		x	x	x	x	x	x	x	[68] (2010)	LS-N	no	–
					63%	53%	66%	38%	69%	88%	75%				

[a] Calendar ageing approximated with cyclic ageing data.

cells in V2X and state that DoD has little effect. The authors entirely omit the effect of DoD dependency in their model. In [18], the authors find a small decrease in battery degradation when applying Load Shifting without optimization (LS-N) to LFP/Gr batteries, while the same conditions for an NCA/Gr battery result in increased battery degradation, showing that NCA/Gr is more sensitive to cyclic ageing than LFP. In a 2020 study of Darcovich et al. [2], the authors revisit a study from 2017 [11] and compare the results to newer, second-generation vehicles. The authors conclude that the costs for second-generation EVs are much lower than those of first-generation batteries, making V2X interesting for EV owners. The lifetime of second-generation EVs used for V2X charging approaches the average car lifetime of 14 years. This highlights that battery technology is developing quickly and can have a large effect on the profitability of V2X. Considering V2X charging during the battery design can improve the impact from V2X.

Key takeaways.

- LFP and NCA have lower average degradation compared to NMC and NMC-LMO
- High DoD increases degradation for NMC cells, while the effect is low for LFP cells
- Newer second-generation batteries have lower degradation, improving the benefit of V2X

4.4. V2X service

Another significant influence is the provided V2X service. This section discusses the degradation impact of frequency services, Peak Shaving, and Load Shifting. The regularity with which the V2X service is delivered has a large impact on the degradation effects [8]. In some studies, the authors allow V2X operation whenever the EV is plugged in, while others mention discrete V2X events [8,11].

Table 3
Yearly degradation reported in V2G degradation studies providing Frequency Containment Reserve (FCR).

Study	Year	Location	Battery type	ΔSoH_{yr}^{V2X}	Yearly profit
Harnischmacher et al. [15]	2023	DE	LFP	0.7%	–
Gehbauer et al. [9]	2023	US-CA	NMC-LMO	–	2.3% ROI
Carmeli et al. [139]	2022	IT	NMC	0.75%	–
Bhoir et al. [13]	2021	UK[a]	NMC	0.155%	6.6% ROI
Calearo and Marinelli [16]	2020	DK	NMC-LMO	0.12%	€-1100/+€700[b]
Calearo and Marinelli [16]	2020	DK	NMC-LMO	0.27%	€-1380/+€700[b]
Calearo and Marinelli [16]	2020	JP	NMC-LMO	0.2%	€-1300/+€700[b]
Baure and Dubarry [150]	2020	US-HI	NCA	0%	–
Tamura [7]	2020	JP	?	0.26%–10.7%	–
Tchagang and Yoo [28]	2020	US (PJM)	?	–	9% saving[c]
Jafari et al. [157]	2018				
Wang et al. [8]	2016	US-CA	NMC-LMO	0.38%	–

[a] UK grid frequency data was used.
[b] The profits for [16] are given for both domestic / industrial prices.
[c] Monetary savings on the energy bill for EV charging.

Table 4
Resulting degradation with different dead-band and frequency spread from [7] at a middle SoC of 0.9 and charging power of 2kW.

	Δf 0.2	Δf 0.1
f_{DB} 0.05	2.10%	6.19%
f_{DB} 0.1	0.46%	

4.4.1. Frequency services

Both FCR and FFR are investigated in V2G degradation studies. Table 3 presents the added degradation due to FCR. The influence of FCR on battery degradation is limited but in all cases positive. In [150], the authors measure no significant added degradation when performing FCR with an NCA cell. Similar results have been found for NMC [13,139], LFP [15] and NMC-LMO [8]. The degradation stays below 0.8% added degradation except for the study of Tamura [7]. In [7], the authors simulate the degradation of battery cells due to FCR in Japan. The authors investigate the influence of the droop characteristic on the degradation of the battery. With an $f_{Deadband}$ of 0.1 Hz and an f_{max} of 0.2 Hz, the degradation can be reduced to as low as 0.26% by limiting the charging current to 1 kW. However, when $f_{Deadband}$ and f_{max} are decreased to 0.05 Hz and 0.1 Hz, the degradation is increased to 10.7% per year, resulting in a lifetime of 1.3 years. The authors use an exponential model from [153] based on a 1998 Nissan Altra and assuming a maximum battery lifetime of 5 years. The absolute results are strongly influenced by this assumption, but the study indicates that the droop characteristic greatly influences the degradation (see Table 4).

In [16], the total profit with industrial prices is significantly higher than domestic prices (€700/yr vs. -€1380/yr). The authors attribute the difference mainly to price difference and charger efficiency, and conclude that V2G with FCR is only profitable with industrial prices. The authors use the efficiency data of a 10 kW charger with very low efficiency at low charging currents. Since the power delivered by FCR is often low, a large amount of energy is lost using the FCR provisioning, affecting the profit. This highlights the importance of efficient converters in the full power range for the intended V2X service. When FCR is applied, large periods of low-power operation can be expected.

As seen in Table 3, the profitability of FCR is relatively low. In [9], the authors mention that providing FCR has little benefit compared to LS-C. In [13], a payback period of 15 years is calculated when only FCR is applied. Between FCR and PS, FCR was the least profitable. In [141], the authors measure the battery degradation with aFRR. Although aFRR is more energy-intensive than FCR, the degradation of both frequency services is similar. Cyclic ageing is increased with aFRR compared to FCR, but calendar ageing is reduced because of the lower average SoC. Since this is only one study, we cannot yet draw general conclusions from it.

Key takeaways.

- Battery degradation with FCR provisioning is limited
- FCR droop characteristic can greatly influence the degradation
- The profit margins of FCR seem small, making battery degradation and storage/conversion efficiency more important
- aFRR seems to cause low degradation too, but more research is needed to verify the results

4.4.2. Peak shaving

Peak shaving will not significantly accelerate battery degradation [8,13,28]. In [28], the authors calculate the charging cost reduction when applying FCR and PS. A cost reduction of 10% can be achieved when applying both FCR and PS simultaneously. The resulting battery degradation is not reported. The effectiveness of PS with V2G is proven by [29], who decreased the demand profile variation by 17% using PS. The authors do not state the amount of added degradation, but the degradation costs are reduced from $18.56 in the uncontrolled case to $7.58 in the controlled V2X case. This is, however, higher than the degradation costs of $5.01 with unidirectional smart charging. In [34], the authors develop an algorithm that optimises charging based on a cost function. The degradation cost is, in almost all cases, increased and in some cases more than doubled, but the authors use a simple cost function that only depends on DoD. In [8], the authors measure battery degradation due to FCR, PS, and LS for NMC-LMO batteries. Even when applied every day, the added degradation from PS is limited to 0.68% per year. This is more than with FCR (0.38%), in contrast with [13,157]. Bhoir et al. [13] measure negligible degradation for FCR and negative degradation for PS, potentially increasing the battery lifetime. Jafari et al. [157] calculate the battery degradation when applying FCR and PS for LFP and conclude that PS results in higher cyclic ageing over time because of the increased energy throughput. However, when the degradation is compared over the energy throughput, FCR results in higher degradation. The amount of added degradation after 100.000 miles is 2% and 3.2% for PS and FCR, respectively. The difference between [8,13,157] can be explained by the fact that [13,157] include the SoC dependency of calendar ageing. Because PS will decrease the average SoC of the battery, the degradation is lower. This highlights the importance of including SoC in the model.

Key takeaways.

- PS has little impact on degradation and can potentially increase the lifetime.
- PS appears to result in lower degradation than FCR.

4.4.3. Load shifting

The results for Load Shifting (LS) are scattered. The degradation results from these services can be seen in Fig. 8. The colour represents

Table 5
Yearly battery degradation due to Load Shifting (LS) where the added degradation is higher than 1%.

Source	Year	Battery type	ΔSoH_{yr}^{V2X}	Δt_{life}	Discussion
Gehbauer et al. [9]	2023	NMC-LMO	1.7%		Only Calendar ageing Temp
Wei et al. [10]	2022	NMC	2%		Large DoD, Daily cycling
Darcovich et al. [14]	2021	NMC	1.7%		Low temperature, 50kW charger
Lim et al. [12]	2021	NMC	1.3%		Changing calendar time
Dubarry et al. [155]	2017	NCA	3.26%		Accelerated cycle testing
Wang et al. [8]	2016	NMC-LMO	2.18%		Daily Load Shaping
Bishop et al. [6]	2013	LFP	25%		Arrhenius Eq. for cyclic ageing Daily RMS value for C-rate and DoD No Calendar ageing

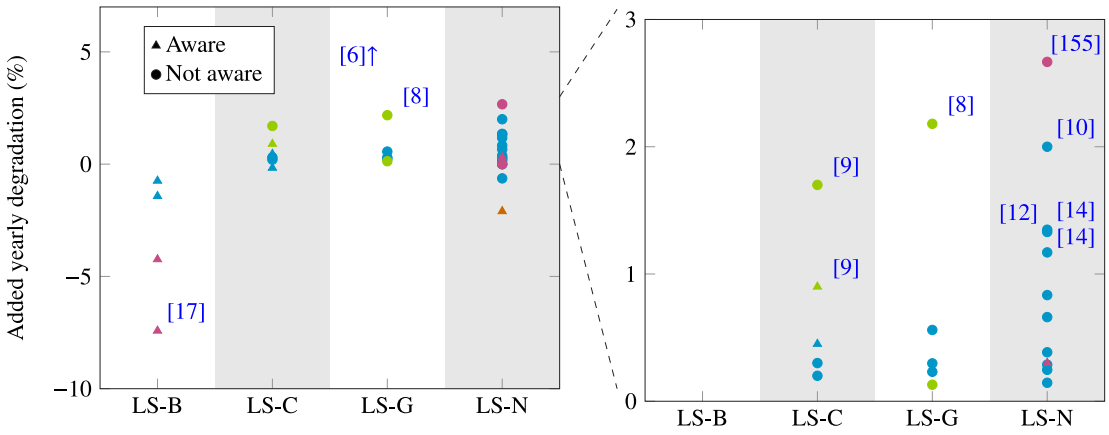

Fig. 8. Degradation results from the literature for all Load Shifting services. The y-axis shows the added yearly degradation, the color of the dot represents the used cathode chemistry, and the shape of the dot indicates if the optimization was ageing aware.

the cathode chemistry, and the shape indicates whether battery ageing was considered in the optimisation. Table 5 shows the articles that found a yearly added degradation above 1%.

LS-B. Fig. 8 shows that the battery lifetime can be successfully reduced when LS-B is applied. In [19], the authors propose a pre-conditioning algorithm that optimises the SoC through V2X. The study does not consider grid requirements. In [17], the authors use a similar method where a trade-off is made between cyclic ageing due to discharging and the decreased calendar ageing at lower SoC. With the proposed optimisation, the battery degradation and the power demand of a building are successfully reduced.

LS-C. One of the most common applications of LS is optimisation for total costs. This has been done in many V2X studies [9,20,29,42,137,144,145]. Many of the sources include battery degradation in the optimisation [9,20,29,42,144,145], some do not [9,137]. Yearly added degradation is limited to 0.9% when degradation costs are included in the optimisation problem. In [9], the authors use Model Predictive Control (MPC) to optimise the charging profile. The MPC controller is defined with and without degradation in the cost function. When degradation is considered, the added degradation from V2B is reduced from 1.7% to 0.9% while the return on investment is increased from 60.8% to 106%. The degradation in Fig. 8 is relatively high. This high degradation is mainly attributed to the use of an NMC-LMO model. The model is simplified by disabling the cyclic ageing effects. This results in a model that only depends on calendar ageing and indirectly on cycling by cell heating.

LS-G. When looking at the column for grid-optimised Load Shifting (LS-G), two data points from [8] stand out. In [8], the degradation of NMC-LMO batteries due to V2X charging is simulated using the model from [101]. Two reasons can be found for the high degradation. Firstly, the NMC-LMO has a shorter lifespan and is more sensitive to cycling than other chemistries. This can also be seen in [9], where the same degradation model was implemented. The second and most important reason is the implementation of Load Shifting in the study. The authors perform Load Shaping so that the fluctuation in load demand is minimised. The EV is charged and discharged continuously to match the demand profile, causing a high cycle count and large energy throughput. When this load profile is applied daily, the added yearly degradation is 2.18%. Load shaping methods which cause continuous and repetitive charge–discharge cycles should be avoided for V2X applications. As mentioned before, the 2013 study of Bishop et al. [6] simulates an exceptionally high degradation of 25% per year, reducing the lifetime of the battery to 1 year when applying V2X. The authors simulate the degradation using the LFP model from [88] with daily RMS, C-rate, and DoD values and high energy throughput. Because the outcome is a clear outlier, it is not included in the results. The results from [6] are often cited to indicate the high impact of V2G on battery degradation [4,17].

LS-N. In [14], the authors simulate the battery degradation of NMC cells in cold weather conditions. The authors simulate two EV models with 28 kWh and 60 kWh batteries and measure the impact of L2 (6.6 kW) and L3 (50 kW) fast charging. The degradation was most significant when applying V2X with an L3 charger to the 28 kWh EV. The high degradation can be attributed to the high charging current under cold temperatures. In [12], the degradation difference between V0X and V2X was relatively high (1.3%). The authors study the battery degradation of real cells by applying Standard Charging (V0X), Smart Charging (V1X), and Vehicle to Everything (V2X) profiles to the cells. Two reasons can be cited for the measured degradation difference. Firstly, the charging profiles of all cases have different lengths. The duration of the V0X profile is 18 h, while the V1X and V2X profiles are 21 h and 24 h. Since the degradation is measured after a fixed number of cycles, the total period of V2X will be 25% longer than the period of V0X, causing an imbalance in the effect of calendar ageing. In [10], the authors measured an added degradation of 2.44% when applying LS-N. The high degradation is mainly attributed to the high DoD between 20% and 100%.

Key takeaways.

- When optimising for battery degradation using LS-B, the battery lifetime can be increased using V2X
- When ageing is included in any optimisation, yearly degradation is limited
- Load shaping methods with continuous and repetitive charge–discharge cycles should be avoided, as they result in high throughput and DoD.
- Large DoD cycles should be avoided

4.4.4. Renewable energy storage

By adding solar generation to the energy system, the benefit of V2X can be increased by allowing the EV to store PV power for later use. In [9,42,137], the charging optimisation accounts for solar generation, but the influence of solar generation is not directly linked to V2X or battery degradation. In [157], the authors calculate the degradation when using V2X as solar storage. The authors measure significant added degradation because of the increased SoC during the day. This indicates that added solar can increase degradation due to high resting SoC when charging is not optimised for battery degradation. A comparison of battery degradation with high amounts of solar and low amounts of solar (e.g. summer vs winter) would give a great insight into the impact of PV on battery degradation.

Key takeaways.

- Using V2X for solar storage can increase degradation due to high SoC during the day, increasing calendar ageing during the day
- More research is needed to evaluate the influence of solar on the battery degradation

4.5. Charging power

Increasing the charging power of the V2X charger will have two influences on battery degradation. Firstly, the C-rate of the cells will increase, which can increase the battery temperature. Secondly, a higher current allows more energy throughput in the same charging time, potentially causing deeper DoD cycles when supporting the grid. As with single cells, the charging and discharging C-rate affect the battery degradation in V2X. As discussed in Section 3.2.3, the effects differ with battery chemistry. NMC and LFP cells show increased degradation with higher currents. The NMC cell is more sensitive to charging current, while the LFP cells are more sensitive to discharging current. The influence of discharge current is unclear for the NCA cells. Some studies [17,132,133] have shown that the degradation increases with low discharge currents, while other studies [134] show the opposite. These differences can also be traced back to the outcome of V2X studies.

In [8,14], the authors model the battery degradation of NMC-LMO and NMC, respectively, and encounter accelerated degradation when using higher charging powers in V2X. In contrast, Uddin et al. [17] perform a V2X degradation study on NCA batteries where the degradation is increased with lower charging currents.

As well as the dependence on chemistry, the effect of charging current also changes heavily with temperature. Battery cells are more prone to effects like lithium plating and particle cracking in cold conditions and with high charging currents. In [14], the L3b (50 kW) charger resulted in higher degradation than the L2b (6.6 kW), but the influence is limited in the case of garage charging. This can be attributed to the elevated temperature during garage charging, which decreases Lithium Plating. In [8], Wang et al. simulate the battery degradation with L1 (1.4 kW) and L2 (7.2 kW) charging using NMC-LMO cells. With an L2 charger, the DoD cycles become significantly deeper, causing increased energy throughput and thus increased degradation. When Load Shifting with Grid optimization (LS-G) is applied daily, the battery's lifetime is decreased from 9.5 to 5 and 3.4 years for L1 and L2 charging, respectively. When LS-G is applied 20 times per year, the lifetime is reduced to 9.2 and 8.8 years for L1 and L2 charging, respectively. The main reason for the high degradation is the large energy throughput. The load profile in [8] includes two discharge cycles from 80%–95% SoC down to 15% SoC, i.e. two full battery discharges per day. With both FCR and PS, the impact of an L2 charger is low. Daily FCR charging decreases the lifetime from 9.5 years down to 8.9 and 8.3 years for L1 and L2, respectively [157]. Measure L1 and L2 chargers and notice no additional degradation. In [142], the authors simulate the degradation for different charging powers. Although the degradation increases with a higher power, the degradation will reach a plateau of around 1.3% degradation.

Key takeaways.

- Increased charging power can decrease battery lifetime, owing to higher C-rate, temperature, and Ah throughput
- High charging power must be avoided during low temperatures, or battery thermal management must be active during V2X provisioning.
- The profitability of V2X in cold weather, when thermal management is enabled, has not yet been investigated.

4.6. Battery size

The effect of battery size is analysed from V2X degradation sources [9,11,14,147] and results are shown in Table 6. In [11,14,147], the authors notice decreasing degradation with increasing battery size, which is in line with the known influence of C-rate and DoD on NMC batteries. In a 2023 study of Gehbauer et al. [9], the authors measure the degradation impact of V2X on two different Nissan Leaf versions. The authors used a 24 kWh version from 2012 and a 60 kWh version from 2022, both with the NMC-LMO/Gr model from Wang et al. [101]. The authors measure higher degradation with the 60 kWh version, contrasting what would be expected from an NMC-LMO cell. There are two main reasons for this contradiction. Firstly, the charging power for the 60 kWh battery is significantly higher than the power used for the 24 kWh version. Secondly, the authors use a semi-empirical degradation model from [101] and omit the dependency on DoD entirely. The studies above only consider NMC and NMC-LMO cathodes. Since the influence of DoD differs from LFP cells, the relation between degradation and battery size might differ with LFP cells compared to NMC. The influence on LFP cells will likely be insignificant, but this remains an open question.

Key takeaways.

- Bigger battery size decreases the impact of V2X on the lifetime of NMC batteries due to lower C-rate and DoD cycles
- The influence of battery size on LFP degradation is not verified

4.7. Degradation models

As shown in Table 2, mainly semi-empirical models were used. Lee et al. [140] are the only authors using a physics-based degradation model to assess the battery degradation. To speed up the simulation, the degradation is accelerated by squeezing one week into 24 h. The authors simulate only the SEI layer growth and overlook other degradation phenomena. The parameters that are considered in the degradation models are shown in Table 2 with an x. The percentage of studies that consider that parameter is shown in the table below. The used models vary greatly in complexity. Some studies only consider Ah throughput, and some include all parameters.

It can be seen that the impact of SoC is often overlooked. The impact of SoC on calendar ageing is included in 53% of the models, while the impact on cyclic ageing is only considered 38% of the time.

Many of the studies depend on degradation models that represent older-generation batteries. The model from [101] is used in 5 sources

Table 6
Battery degradation due to V2X for different battery sizes. In case of [147], the battery lifetime loss is presented.

Source	Battery Size	Charging Power	Lifetime
Darcovich et al. [11]	28kWh	6.6kW	8.5
	42kWh	6.6kW	10.2
	70kWh	6.6kW	12
Darcovich et al. [14]	28kWh	6.6kW	7.7
	65kWh	6.6kW	10.4
Gehbauer et al. [9]	24kWh	15kW	5
	60kWh	50kW	2.9
Li et al. [147][a]	37kWh	–	−8.4%
	53kWh	–	−6.2%
	69kWh	–	−5.5%

[a] Li et al. give a lifetime reduction in per cent when providing V2X.

and is used as a base for other models [8,104]. This model is for an NMC-LMO cathode from 2014, an old chemistry used in the first-generation Nissan Leafs. Battery technology has since come a long way. Similarly, in [7], the authors use a model from [153] based on a 1988 Nissan Altra, resulting in very high degradation results. In a 2020 study of Darcovich et al. [2], the authors revisit a study from 2017 [11] and compare the old results to newer, second-generation vehicles. The authors conclude that the lifetime of second-generation EVs used for V2X charging approaches the average car lifetime of 14 years.

The models from Wang et al. [101] (NMC-LMO) and Wang et al. [88] (LFP) are often used and cited in V2X studies. Calendar and cyclic ageing are included in the studies. In the model of Wang et al. [101], the authors did not perform a calendar ageing test but derived the calendar ageing parameters from the nearest possible cyclic data with a DoD of 10% and a current of C/2. This can greatly distort the degradation outcome. Time resolution is another important parameter of the degradation model. Most degradation studies have a time step of 1 s [8,13,19,29,139,144]. Some models have time steps up to 5 min [15,34] or even 15 min [28]. In [6], the degradation is calculated for a 24 h average. This creates large errors in the degradation calculations. To accurately assess battery degradation with fast-changing power profiles, it is important to use small time steps in the simulation.

Key takeaways.

- The influence of SoC is often overlooked
- High presence of the model from [101] with limited calendar ageing data
- Models used to assess battery degradation should be based on newer generation batteries
- Time averaging should be avoided, but most models consider proper time resolution

4.8. Optimising to reduce battery ageing

Optimising the energy dispatch with the inclusion of battery degradation is a hard task since battery degradation is highly nonlinear. To solve this issue, models are often linearised, or stress factors are excluded. This section presents a review of degradation models in V2X optimisation. In Table 7, the included stress factors are listed.

Among the most complete models in Table 7 are [9,17,19], and [142]. In the article from Khezri et al. [142], the authors use an Mixed-Integer Linear Programming optimisation based on the model of Wang et al. [101]. Because [101] does not include SoC dependency in the calendar ageing model, Khezri et al. integrate the SoC dependency from [52]. The authors use a piecewise linear function to model the SoC dependency. In [9], the authors also use a linearised version of Wang et al. [101] to estimate the battery degradation. The linear model is implemented into an Mixed-Integer Linear Programming model. The model is linearised around the current operating point to allow optimisation into the short future. This method simplifies the optimisation in return for small linearisation errors. The shortcomings of this method are that the accuracy depends on the timestep length, and the impact of SoC on calendar ageing is not accounted for in the optimisation. A similar method is used in [144] where the optimisation does not account for SoC too, neglecting potential calendar ageing effects. In [17,19], the optimisation algorithm does not optimise the charging pattern but finds the optimal SoC to rest. The algorithm determines the calendar ageing for each SoC value and the amount of cyclic ageing from (dis)charging to that SoC. Then, the EV will (dis)charge to the SoC with the lowest total ageing. Both authors prove that V2X can improve the battery lifetime by optimising the resting SoC. The SoC is a largely overlooked stress factor in the optimisation of degradation. Only [142] includes the SoC in a full optimisation model. [17,19] optimise the resting SoC but do not optimise other factors.

Key takeaways.

- The SoC is a largely overlooked stress factor in the optimisation of degradation

4.9. Thermal management and modelling

The last column of Table 2 indicates the thermal model used in the study. Only a few studies consider battery heating. [8,9,16,17,139] all model the thermal behaviour of the battery using an RC thermal model. When a cell is cycled at low temperatures, the chance of lithium plating and particle cracking increases [159], which is also measured in V2X degradation studies [14]. Both cases illustrate the importance of considering thermal management when performing battery degradation studies and when optimising the V2X charging current. To avoid excessive degradation, the charging power needs to be adapted to the thermal conditions of the cell by limiting high charging currents at low temperatures to avoid lithium plating. In [157], the authors calculate the degradation for three different climates. The degradation was found to be higher in hotter climates, most likely because of higher calendar ageing effects. The difference between the cold climate and the two hot climates is 2.23% and 2.83% yearly degradation. The authors compare the degradation with active and passive thermal management and conclude a difference of 1.14%.

Key takeaways.

- Thermal models are often overlooked in V2X degradation models, neglecting one of the most important parameters in battery degradation
- Active thermal management can decrease degradation by V2X by heating the battery during operation
- Added V2X cycles at low temperatures without thermal management cause higher degradation

Table 7
Stress factors included in degradation models for V2X optimisation.

Study	Calendar			Cyclic				
	t	T	SoC	T	SoC	DoD	C-rate	Ah
Visakh and Selvan [29]						x	x	
Zheng et al. [144]			–		x		x	
Manzolli et al. [145]							x	x
Gehbauer et al. [9]	x	x		x			x	x
Ginigeme and Wang [34]						x		
Uddin et al. [17]	x	x	x	x	x	x	x	x
Bui et al. [19]	x	x	x	x			x	x
Tchagang and Yoo [28]						x	x	
Khezri et al. [142]	x	x	x	x			x	x
Lee and Kim [158]	x		x					

4.10. Locality

The locality has a large influence on battery degradation through climate conditions and driving habits. In Section 2, the importance of battery temperature was highlighted. High battery temperatures increase calendar ageing [47], but increase cyclic ageing to a lesser extent [159]. Therefore, hot climates are expected to change the ageing ratio between calendar and cyclic ageing, making V2X more attractive. In a 2015 study of Marongiu et al. [32], the authors study the degradation of NCA and LFP cells in Aachen (DE) and Dubai (AE) with average ambient temperatures of 10.3 °C and 27.1 °C respectively. The authors calculate the operational costs for both locations and conclude that the ambient temperature has a limited impact on the degradation of V2X. In the hotter climate of Dubai, V2X can compensate for some of the calendar ageing costs at high temperatures, making it more attractive. The authors do not review the added value of V2X when it is used to optimise degradation by adjusting the SoC. In [14], the authors measure the degradation with V2X in different cold climate cities in Canada. The authors modelled the battery cells using a thermal model of a prismatic cell. The authors conclude that there is an increased degradation in colder climates. In [160], the authors perform two case studies for Sweden and Spain, but they use a simplified linear degradation model. Likewise, in a recent study of [161], the authors propose a techno-economical analysis for V2X in cold climate countries while not considering ambient temperature in their degradation model.

Key takeaways.

- Higher ambient temperatures will likely increase the benefit of V2X, as high battery temperatures increase calendar ageing but decrease cyclic ageing
- More research is needed to investigate the benefit of V2X in different climates while considering the operation of the thermal management system

4.11. Reduce battery degradation

In some studies [10,17–20], the authors prove that V2X can be used to reduce battery degradation. Uddin et al. [17] were the first to propose this in 2017. The authors use a detailed semi-empirical model for NCA cells, taking calendar ageing and cyclic ageing into account. The optimisation algorithm calculates the degradation at the arrival SoC_i and compares this to the degradation from storing at any other SoC_{i+1} plus the degradation due to cycling to SoC_{i+1}. When it finds a SoC where the calendar and cyclic degradation are less, it discharges to SoC_{i+1}. The car is charged back to the required SoC before departure. When the peak load of the building is too high, the algorithm applies peak shaving to the cars that can benefit from V2X. This algorithm works well for reducing battery degradation and can reduce peak power demand. In [10], the authors perform a degradation study on NMC cells where they cycle the battery with different DoD at different middle SoC values. The authors conclude that the battery degradation can be reversed when the resting SoC is lowered from 90%–100% to 65%. The authors do not consider the grid's needs. In [19], Bui et al. propose a pre-conditioning method, where they lower the battery SoC with V2X to decrease calendar ageing like in [17]. The authors measure the battery degradation on real cells and can decrease the battery degradation when the cells are new. However, when cells are aged, the optimisation algorithm is not capable of decreasing the battery degradation. This is most likely because the degradation model in the optimisation algorithm is not accurate enough. It is useful to perform long-term degradation studies in future research. In a 2024 study by [142], the authors implement LS-C and LS-B. In the case of LS-C, the authors implement an optimisation with and without degradation included. In all cases, the degradation is reduced compared to uncontrolled charging. In the case of LS-C, the degradation is not reduced compared to V1X with delayed charging, but in the case of LS-B, the yearly degradation is reduced to 0.60%. The studies show that V2X can be very promising to lower battery degradation, but the benefit over smart charging (V1X) and the benefit for the grid operator should be investigated further.

Key takeaways.

- V2X can decrease battery degradation by lowering the SoC during resting, thereby reducing calendar ageing like SEI formation
- The benefit of V2X over V1X for battery degradation should be examined more, as most studies compare V2X ageing to uncontrolled charging, where there is high calendar ageing as EVs are generally left at high SoC during parking periods

4.12. Benefit of V2X over V1X

To reduce grid peak demand and grid load variation, smart charging (V1X) or delayed charging has already proven to be highly beneficial. Because V2X requires a charger upgrade to allow bi-directional current, the benefit of V2X over V1X is still debated. In this section the degradation benefits of V2X over V1X are compared. Results are shown in Table 8. In [8,9,19,29,137,142] both V1X charging and V2X charging were considered. In [8,9,137], the authors simulated that the degradation will increase significantly when providing V2X instead of V1X. In [8], FCR, PS, and Load Shaping were considered. In [29], the authors calculate degradation costs of $5.01 for the V1X and $7.58 for the V2X case when applying PS. The only study claiming that degradation is reduced when applying V2X over V1X is [19]. In [19], the authors used a charging profile optimised for battery degradation. The study shows the opportunity of V2X to decrease degradation compared to V1X, but this has to be validated for more scenarios. In [142], the authors simulate a higher degradation for V2X compared to V1X, but the operational costs are decreased by 74%. Furthermore, the authors simulated with degradation optimisation (LS-B) and decreased the yearly degradation to 0.60%. Another factor that can influence the benefit of V2X over V1X is the arrival State of Charge (SoC). The arrival SoC is influenced by the DoD due to driving (ΔDoD_{drive}). When considering a commuter

Table 8
The absolute degradation values or costs when applying Standard Charging (V0X), Smart Charging (V1X), and Vehicle to Everything (V2X).

Source	Service	V0X	V1X	V2X
Wang et al. [8]	FCR	–	3.12%	3.5%
Wang et al. [8]	PS	–	3.12%	3.8%
Wang et al. [8]	LS-G	–	3.12%	5.3%
Englberger et al. [137]	LS-C	2.0%	2.2%	2.4%
Bui et al. [19]	LS-B	8.62%	8.59%	7.88%
Visakh and Selvan [29]	PS	–	$5.01	$7.58
Khezri et al. [142]	LS-C	3.16%	0.97%	1.23%
Khezri et al. [142]	LS-B	3.16%	0.97%	0.60%

car, the profitability of V2X will be influenced by the commuting distance. In [17], the authors simulate the degradation of 120 EVs with different commuting distances. When the SoC reduction due to driving ΔSoC_{drive} is between 21% and 38%, the capacity and power fade can be reduced using V2X charging. With low arrival SoC, the calendar ageing is already low enough, so discharging through V2X would have limited benefits. On the other hand, with very high arrival SoC, the degradation due to cycling could be higher than the benefit of decreased calendar ageing. More research on the influence of arrival SoC is necessary.

Key takeaways.

- V2X can increase or decrease degradation compared to V1X but more research is needed to investigate the benefit of V2X over V1X
- More research on the influence of arrival SoC is necessary.

4.13. Social challenges

In [3], the authors perform an extensive review of interviews on the topic of V2X charging. The interviewees do not consider battery degradation a technical challenge but rather a social challenge. In a questionnaire for EV users that used V2X [5], twelve out of seventeen interviewees mentioned battery degradation. They were questioning how the amount of degradation was compared to degradation due to driving, and what amount of compensation would be reasonable for the use of their battery. Communication is a large factor in convincing EV users and EV users show more trust in their OEMs for information [3]. This shows that communication of the OEM is of utmost importance to convince users of the benefits and risks.

Key takeaways.

- Battery degradation is a concern for EV users that consider using V2X
- Car OEMs are important in communication about V2X

5. Conclusion

Battery degradation remains one of the biggest concerns for EV users when considering V2X. In this review, we quantitatively compared the battery degradation results of 37 V2X studies. The V2X degradation studies give conflicting results. Some studies claim that V2X is detrimental to battery lifetime, while others claim that V2X can extend the battery lifetime. An attempt was made to compare all degradation studies and address the contradictions by referring to battery degradation theory. The added yearly degradation by V2X is between 0.35% and 1.4%. Most of the contradictions can be ascribed to the following four categories.

Battery chemistry. Differences in chemistries can have a large effect on the degradation. When comparing battery chemistries, NCA and LFP cathodes have lower degradation than batteries with NMC cathodes. The age of the battery is also an important parameter. Newer cells have lower cyclic ageing compared to calendar ageing, making the impact of V2X lower. Many of the degradation models in current V2X literature depend on old battery chemistries like NMC-LMO or older NCM cells, causing a large overestimation of the degradation.

V2X service. The provided service can have a big impact on degradation. Especially the C-rate, DoD, and frequency of use are important parameters. Literature has shown that degradation can be limited when small DoD and low C-rates are applied. When the SoC is lowered using Peak Shaving or Load Shaping, the battery lifetime can even be increased. Services that cause the SoC to rise, like solar storage applications, can cause the degradation to increase. More research is needed in this field to estimate the impact of solar storage using V2X. Providing V2X services during cold temperatures without thermal management should be avoided.

Degradation model. An important factor in the degradation results is the degradation model. Almost all studies use a semi-empirical degradation model. Temperature and SoC are the most overlooked stress factors in the V2X degradation models. Many studies rely on degradation models based on older-generation batteries. Few studies have included thermal models of the battery to model cell heating. By omitting the effect of SoC, the impact of V2X on degradation will be overestimated.

Optimisation. When any form of degradation is included in the optimisation of the V2X profile, the added degradation can be limited to 0.9% per year. Many optimisation methods ignore the effect of SoC on battery degradation, leaving a large opportunity for improvement. When optimisation is targeted for battery degradation, V2X can extend the battery lifetime. More research is needed to prove the benefit of V2X over V1X.

Implications. The findings of this review carry significant implications for the advancement and deployment of V2X technology. While the average added yearly degradation from V2X is low, the wide spread across studies highlights a lack of consensus. This inconsistency is a challenge to both industry stakeholders and policymakers, because user acceptance depends on it.

Future research should focus on new generation EV batteries with more accurate models that include the effects of Temperature and State of Charge. Authors should try to avoid degradation models that are based on old battery types like NMC-LMO. The insight that any optimisation, simple or sophisticated, can significantly limit the degradation provides an opportunity for further research in the optimisation of V2X services.

CRediT authorship contribution statement

Koen Linders: Writing – original draft, Resources, Project administration, Methodology, Formal analysis, Data curation, Conceptualization. **Samppa Jenu:** Writing – original draft, Investigation, Formal analysis, Data curation. **Ari Hentunen:** Writing – original draft, Investigation, Formal analysis, Data curation . **Gautham Ram Chandra Mouli:** Writing – review & editing, Project administration, Methodology, Funding acquisition, Conceptualization.

Declaration of competing interest

The authors declare that they have no known competing financial interests or personal relationships that could have appeared to influence the work reported in this paper.

Acknowledgements

The collaboration for this article was established through the networking efforts of Dr. Goncalo Pinto Mendes and Prof. Pertti Kauranen from LUT University. The authors would also like to thank Prof. Pertti Kauranen for his expert opinion on sections 2 and 3. Finally, many thanks to Prof. Pavol Bauer for the discussions on the content of the article.

This project has received funding from the European Union's Horizon Europe research and innovation programme under grant agreement No 101056934. This project has received funding from the UK Research and Innovation agency (UKRI). Reference number: 10055673

Data availability

Data will be made available on request.

References

[1] N.S. Pearre, W. Kempton, R.L. Guensler, V.V. Elango, Electric vehicles: How much range is required for a day's driving? Transp. Res. Part C: Emerg. Technol. 19 (6) (2011) 1171–1184, http://dx.doi.org/10.1016/j.trc.2010.12.010.

[2] K. Darcovich, T. Laurent, H. Ribberink, Improved prospects for V2X with longer range 2nd generation electric vehicles, ETransportation 6 (2020) 100085, http://dx.doi.org/10.1016/j.etran.2020.100085.

[3] C. Gschwendtner, S.R. Sinsel, A. Stephan, Vehicle-to-X (V2X) implementation: An overview of predominate trial configurations and technical, social and regulatory challenges, Renew. Sustain. Energy Rev. 145 (2021) 110977, http://dx.doi.org/10.1016/j.rser.2021.110977.

[4] A.W. Thompson, Economic implications of Lithium Ion battery degradation for Vehicle-to-Grid (V2X) services, J. Power Sources 396 (2018) 691–709, http://dx.doi.org/10.1016/j.jpowsour.2018.06.053.

[5] R. Ghotge, K.P. Nijssen, J.A. Annema, Z. Lukszo, Use before you choose: what do EV drivers think about V2G after experiencing it? Energies 15 (13) (2022) 4907, http://dx.doi.org/10.3390/en15134907.

[6] J.D. Bishop, C.J. Axon, D. Bonilla, M. Tran, D. Banister, M.D. McCulloch, Evaluating the impact of V2G services on the degradation of batteries in PHEV and EV, Appl. Energy 111 (2013) 206–218, http://dx.doi.org/10.1016/j.apenergy.2013.04.094.

[7] S. Tamura, A V2G strategy to increase the cost–benefit of primary frequency regulation considering EV battery degradation, Electr. Eng. Japan 212 (1–4) (2020) 11–22, http://dx.doi.org/10.1002/eej.23270.

[8] D. Wang, J. Coignard, T. Zeng, C. Zhang, S. Saxena, Quantifying electric vehicle battery degradation from driving vs. vehicle-to-grid services, J. Power Sources 332 (2016) 193–203, http://dx.doi.org/10.1016/j.jpowsour.2016.09.116.

[9] C. Gehbauer, D.R. Black, P. Grant, Advanced control strategies to manage electric vehicle drivetrain battery health for Vehicle-to-X applications, Appl. Energy 345 (2023) 121296, http://dx.doi.org/10.1016/j.apenergy.2023.121296.

[10] Y. Wei, Y. Yao, K. Pang, C. Xu, X. Han, L. Lu, Y. Li, Y. Qin, Y. Zheng, H. Wang, M. Ouyang, A comprehensive study of degradation characteristics and mechanisms of commercial Li(NiMnCo)O2 EV batteries under Vehicle-To-Grid (V2G) services, Batteries 8 (10) (2022) 188, http://dx.doi.org/10.3390/batteries8100188.

[11] K. Darcovich, S. Recoskie, H. Ribberink, F. Pincet, A. Foissac, Effect on battery life of vehicle-to-home electric power provision under Canadian residential electrical demand, Appl. Therm. Eng. 114 (2017) 1515–1522, http://dx.doi.org/10.1016/j.applthermaleng.2016.07.002.

[12] J. Lim, S.-E. Lee, K.-Y. Park, H.-S. Kim, J.-H. Choi, VxG pattern-based analysis and battery deterioration diagnosis, Energies 14 (17) (2021) 5422, http://dx.doi.org/10.3390/en14175422.

[13] S. Bhoir, P. Caliandro, C. Brivio, Impact of V2G service provision on battery life, J. Energy Storage 44 (2021) 103178, http://dx.doi.org/10.1016/j.est.2021.103178.

[14] K. Darcovich, S. Recoskie, H. Ribberink, C. Michelet, The impact of V2X service under local climatic conditions within Canada on EV durability, ETransportation 9 (2021) 100124, http://dx.doi.org/10.1016/j.etran.2021.100124.

[15] C. Harnischmacher, L. Markefke, A.B. Brendel, L. Kolbe, Two-sided sustainability: Simulating battery degradation in vehicle to grid applications within autonomous electric port transportation, J. Clean. Prod. 384 (2023) 135598, http://dx.doi.org/10.1016/j.jclepro.2022.135598.

[16] L. Calearo, M. Marinelli, Profitability of frequency regulation by electric vehicles in Denmark and Japan considering battery degradation costs, World Electr. Veh. J. 11 (3) (2020) 48, http://dx.doi.org/10.3390/wevj11030048.

[17] K. Uddin, T. Jackson, W.D. Widanage, G. Chouchelamane, P.A. Jennings, J. Marco, On the possibility of extending the lifetime of Lithium-Ion batteries through optimal V2G facilitated by an integrated vehicle and smart-grid system, Energy 133 (2017) 710–722, http://dx.doi.org/10.1016/j.energy.2017.04.116.

[18] M. Petit, E. Prada, V. Sauvant-Moynot, Development of an empirical aging model for Li-ion batteries and application to assess the impact of Vehicle-to-Grid strategies on battery lifetime, Appl. Energy 172 (2016) 398–407, http://dx.doi.org/10.1016/j.apenergy.2016.03.119.

[19] T.M.N. Bui, M. Sheikh, T.Q. Dinh, A. Gupta, D.W. Widanalage, J. Marco, A study of reduced battery degradation through state-of-charge pre-conditioning for Vehicle-to-Grid Operations, IEEE Access 9 (2021) 155871–155896, http://dx.doi.org/10.1109/ACCESS.2021.3128774.

[20] Y. Iwafune, K. Ogimoto, Economic impacts of the demand response of electric vehicles considering battery degradation, Energies 13 (21) (2020) 5771, http://dx.doi.org/10.3390/en13215771.

[21] A. Hoke, A. Brissette, D. Maksimović, A. Pratt, K. Smith, Electric vehicle charge optimization including effects of Lithium-Ion battery degradation, in: 2011 IEEE Vehicle Power and Propulsion Conference, 2011, pp. 1–8, http://dx.doi.org/10.1109/VPPC.2011.6043046.

[22] S. Haider, R.e.Z. Rizvi, J. Walewski, P. Schegner, Investigating peer-to-peer power transactions for reducing EV induced network congestion, Energy 254 (2022) 124317, http://dx.doi.org/10.1016/j.energy.2022.124317.

[23] C. Xu, P. Behrens, P. Gasper, K. Smith, M. Hu, A. Tukker, B. Steubing, Electric vehicle batteries alone could satisfy short-term grid storage demand by as early as 2030, Nat. Commun. 14 (1) (2023) 119, http://dx.doi.org/10.1038/s41467-022-35393-0.

[24] S. Nazari, F. Borrelli, A. Stefanopoulou, Electric vehicles for smart buildings: A survey on applications, energy management methods, and battery degradation, Proc. IEEE 109 (6) (2021) 1128–1144, http://dx.doi.org/10.1109/JPROC.2020.3038585.

[25] C. Heilmann, G. Friedl, Factors influencing the economic success of grid-to-vehicle and vehicle-to-grid applications—A review and meta-analysis, Renew. Sustain. Energy Rev. 145 (2021) 111115, http://dx.doi.org/10.1016/j.rser.2021.111115.

[26] A.W. Thompson, Y. Perez, Vehicle-to-Everything (V2X) energy services, value streams, and regulatory policy implications, Energy Policy 137 (2020) 111136, http://dx.doi.org/10.1016/j.enpol.2019.111136.

[27] Fingrid, Frequency containment reserves (FCR products), 2017, https://www.fingrid.fi/en/electricity-market/reserves_and_balancing/frequency-containment-reserves/. (Accessed 5 June 2024).

[28] A. Tchagang, Y. Yoo, V2B/V2G on energy cost and battery degradation under different driving scenarios, peak shaving, and frequency regulations, World Electr. Veh. J. 11 (1) (2020) 14, http://dx.doi.org/10.3390/wevj11010014.

[29] A. Visakh, M.P. Selvan, Feasibility assessment of utilizing electric vehicles for energy arbitrage in smart grids considering battery degradation cost, Energy Sources Part A: Recover. Util. Environmental Eff. 44 (2) (2022) 4664–4678, http://dx.doi.org/10.1080/15567036.2022.2078443.

[30] ACER, ACER market monitoring report 2015 - electricity and gas retail markets, 2016, https://www.acer.europa.eu/sites/default/files/documents/Publications/ACER Market Monitoring Report 2015 - ELECTRICITY AND GAS RETAIL MARKETS.pdf. (Accessed 4 April 2024).

[31] X. Zhang, C.C. Qin, E. Loth, Y. Xu, X. Zhou, H. Chen, Arbitrage analysis for different energy storage technologies and strategies, Energy Rep. 7 (2021) 8198–8206, http://dx.doi.org/10.1016/j.egyr.2021.09.009.

[32] A. Marongiu, M. Roscher, D.U. Sauer, Influence of the vehicle-to-grid strategy on the aging behavior of Lithium battery electric vehicles, Appl. Energy 137 (2015) 899–912, http://dx.doi.org/10.1016/j.apenergy.2014.06.063.

[33] A. Pepiciello, A. Vaccaro, The role of vehicle to grid technology for enhancing power distribution system flexibility, in: 2022 IEEE International Workshop on Metrology for Automotive (MetroAutomotive), 2022, pp. 24–29, http://dx.doi.org/10.1109/MetroAutomotive54295.2022.9855066.

[34] K. Ginigeme, Z. Wang, Distributed optimal vehicle-to-grid approaches with consideration of battery degradation cost under real-time pricing, IEEE Access 8 (2020) 5225–5235, http://dx.doi.org/10.1109/ACCESS.2019.2963692.

[35] N.S. Pearre, H. Ribberink, Review of research on V2X technologies, strategies, and operations, Renew. Sustain. Energy Rev. 105 (2019) 61–70, http://dx.doi.org/10.1016/j.rser.2019.01.047.

[36] P. Kushwaha, V. Prakash, S. Yamujala, R. Bhakar, Fast frequency response constrained electric vehicle scheduling for low inertia power systems, J. Energy Storage 62 (2023) 106944, http://dx.doi.org/10.1016/j.est.2023.106944.

[37] K. Sevdari, L. Calearo, P.B. Andersen, M. Marinelli, Ancillary services and electric vehicles: An overview from charging clusters and chargers technology perspectives, Renew. Sustain. Energy Rev. 167 (2022) 112666, http://dx.doi.org/10.1016/j.rser.2022.112666.

[38] J. Guo, J. Yang, Z. Lin, C. Serrano, A.M. Cortes, Impact analysis of V2G services on EV battery degradation -a review, in: 2019 IEEE Milan PowerTech, 2019, pp. 1–6, http://dx.doi.org/10.1109/PTC.2019.8810982.

[39] T.A. Lehtola, A. Zahedi, Electric vehicle battery cell cycle aging in vehicle to grid operations: A review, IEEE J. Emerg. Sel. Top. Power Electron. 9 (1) (2021) 423–437, http://dx.doi.org/10.1109/JESTPE.2019.2959276.

[40] A. Leippi, M. Fleschutz, M.D. Murphy, A review of EV battery utilization in demand response considering battery degradation in non-residential vehicle-to-grid scenarios, Energies 15 (9) (2022) 3227, http://dx.doi.org/10.3390/en15093227.

[41] P. Zhu, D. Gastol, J. Marshall, R. Sommerville, V. Goodship, E. Kendrick, A review of current collectors for Lithium-Ion batteries, J. Power Sources 485 (2021) 229321, http://dx.doi.org/10.1016/j.jpowsour.2020.229321.

[42] W. Vermeer, G.R. Chandra Mouli, P. Bauer, Real-time building smart charging system based on PV forecast and Li-Ion battery degradation, Energies 13 (13) (2020) 3415, http://dx.doi.org/10.3390/en13133415.

[43] X. Han, L. Lu, Y. Zheng, X. Feng, Z. Li, J. Li, M. Ouyang, A review on the key issues of the Lithium Ion battery degradation among the whole life cycle, ETransportation 1 (2019) 100005, http://dx.doi.org/10.1016/j.etran.2019.100005.

[44] C.R. Birkl, M.R. Roberts, E. McTurk, P.G. Bruce, D.A. Howey, Degradation diagnostics forLithium Ion cells, J. Power Sources 341 (2017) 373–386, http://dx.doi.org/10.1016/j.jpowsour.2016.12.011.

[45] S.E.J. O'Kane, W. Ai, G. Madabattula, D. Alonso-Alvarez, R. Timms, V. Sulzer, J.S. Edge, B. Wu, G.J. Offer, M. Marinescu, Lithium-Ion battery degradation: How to model it, Phys. Chem. Chem. Phys. 24 (13) (2022) 7909–7922, http://dx.doi.org/10.1039/D2CP00417H.

[46] W. Vermeer, G.R. Chandra Mouli, P. Bauer, A comprehensive review on the characteristics and modeling of Lithium-Ion battery aging, IEEE Trans. Transp. Electrification 8 (2) (2022) 2205–2232, http://dx.doi.org/10.1109/TTE.2021.3138357.

[47] S.J. An, J. Li, C. Daniel, D. Mohanty, S. Nagpure, D.L. Wood, The state of understanding of the Lithium-Ion-battery graphite solid electrolyte interphase (SEI) and its relationship to formation cycling, Carbon 105 (2016) 52–76, http://dx.doi.org/10.1016/j.carbon.2016.04.008.

[48] J.A. Gilbert, I.A. Shkrob, D.P. Abraham, Transition metal dissolution, ion migration, electrocatalytic reduction and capacity loss in Lithium-Ion Full Cells, J. Electrochem. Soc. 164 (2) (2017) A389, http://dx.doi.org/10.1149/2.1111702jes.

[49] J. Vetter, P. Novák, M.R. Wagner, C. Veit, K.C. Möller, J.O. Besenhard, M. Winter, M. Wohlfahrt-Mehrens, C. Vogler, A. Hammouche, Ageing mechanisms in Lithium-Ion batteries, J. Power Sources 147 (1) (2005) 269–281, http://dx.doi.org/10.1016/j.jpowsour.2005.01.006.

[50] A.J. Warnecke, Degradation Mechanisms in NMC-Based Lithium-Ion Batteries, RWTH Aachen University, 2017, http://dx.doi.org/10.18154/RWTH-2017-09646, volume RWTH Aachen University.

[51] W. Ai, B. Wu, E. Martínez-Pañeda, A coupled phase field formulation for modelling fatigue cracking in Lithium-Ion battery electrode particles, J. Power Sources 544 (2022) 231805, http://dx.doi.org/10.1016/j.jpowsour.2022.231805.

[52] P. Keil, S.F. Schuster, J. Wilhelm, J. Travi, A. Hauser, R.C. Karl, A. Jossen, Calendar aging of Lithium-Ion batteries, J. Electrochem. Soc. 163 (9) (2016) A1872, http://dx.doi.org/10.1149/2.0411609jes.

[53] B. Li, Y. Chao, M. Li, Y. Xiao, R. Li, K. Yang, X. Cui, G. Xu, L. Li, C. Yang, Y. Yu, D.P. Wilkinson, J. Zhang, A review of solid electrolyte interphase (SEI) and dendrite formation in Lithium batteries, Electrochem. Energy Rev. 6 (1) (2023) 7, http://dx.doi.org/10.1007/s41918-022-00147-5.

[54] T.R. Tanim, Z. Yang, D.P. Finegan, P.R. Chinnam, Y. Lin, P.J. Weddle, I. Bloom, A.M. Colclasure, E.J. Dufek, J. Wen, Y. Tsai, M.C. Evans, K. Smith, J.M. Allen, C.C. Dickerson, A.H. Quinn, A.R. Dunlop, S.E. Trask, A.N. Jansen, A comprehensive understanding of the aging effects of extreme fast charging on high Ni NMC cathode, Adv. Energy Mater. 12 (22) (2022) 2103712, http://dx.doi.org/10.1002/aenm.202103712.

[55] R. Stockhausen, L. Gehrlein, M. Müller, T. Bergfeldt, A. Hofmann, F.J. Müller, J. Maibach, H. Ehrenberg, A. Smith, Investigating the dominant decomposition mechanisms in Lithium-Ion battery cells responsible for capacity loss in different stages of electrochemical aging, J. Power Sources 543 (2022) 231842, http://dx.doi.org/10.1016/j.jpowsour.2022.231842.

[56] L. Wang, J. Qiu, X. Wang, L. Chen, G. Cao, J. Wang, H. Zhang, X. He, Insights for understanding multiscale degradation of LiFePO4 cathodes, EScience 2 (2) (2022) 125–137, http://dx.doi.org/10.1016/j.esci.2022.03.006.

[57] D. Uxa, B. Jerliu, E. Hüger, L. Dörrer, M. Horisberger, J. Stahn, H. Schmidt, On the lithiation mechanism of amorphous silicon electrodes in Li-Ion Batteries, J. Phys. Chem. C 123 (36) (2019) 22027–22039, http://dx.doi.org/10.1021/acs.jpcc.9b06011.

[58] X. Lin, K. Khosravinia, X. Hu, J. Li, W. Lu, Lithium plating mechanism, detection, and mitigation in Lithium-Ion batteries, Prog. Energy Combust. Sci. 87 (2021) 100953, http://dx.doi.org/10.1016/j.pecs.2021.100953.

[59] M. Petzl, M. Kasper, M.A. Danzer, Lithium plating in a commercial Lithium-Ion battery – A low-temperature aging study, J. Power Sources 275 (2015) 799–807, http://dx.doi.org/10.1016/j.jpowsour.2014.11.065.

[60] Q. Liu, C. Du, B. Shen, P. Zuo, X. Cheng, Y. Ma, G. Yin, Y. Gao, Understanding undesirable anode Lithium plating issues in lithium-ion batteries, RSC Adv. 6 (91) (2016) 88683–88700, http://dx.doi.org/10.1039/C6RA19482F.

[61] E. Zhao, L. Fang, M. Chen, D. Chen, Q. Huang, Z. Hu, Q.-b. Yan, M. Wu, X. Xiao, New insight into Li/Ni disorder in layered cathode materials for Lithium Ion batteries: A joint study of neutron diffraction, electrochemical kinetic analysis and first-principles calculations, J. Mater. Chem. A 5 (4) (2017) 1679–1686, http://dx.doi.org/10.1039/C6TA08448F.

[62] J. Zheng, Y. Ye, T. Liu, Y. Xiao, C. Wang, F. Wang, F. Pan, Ni/li disordering in layered transition metal oxide: electrochemical impact, origin, and control, Acc. Chem. Res. 52 (8) (2019) 2201–2209, http://dx.doi.org/10.1021/acs.accounts.9b00033.

[63] M. Lewerenz, A. Marongiu, A. Warnecke, D.U. Sauer, Differential voltage analysis as a tool for analyzing inhomogeneous aging: A case study for LiFePO4 | graphite cylindrical cells, J. Power Sources 368 (2017) 57–67, http://dx.doi.org/10.1016/j.jpowsour.2017.09.059.

[64] IEA, Trends in batteries – global EV outlook 2023, 2023, https://www.iea.org/reports/global-ev-outlook-2023/trends-in-batteries. (Accessed 17 August 2023).

[65] T. Gross, How 'modern-Day Slavery' in the Congo powers the rechargeable battery economy, 2023, https://www.npr.org/sections/goatsandsoda/2023/02/01/1152893248/red-cobalt-congo-drc-mining-siddharth-kara. (Accessed 9 August 2023).

[66] H. Darjazi, E. Gonzalo, B. Acebedo, R. Cid, M. Zarrabeitia, F. Bonilla, M.Á. Muñoz-Márquez, F. Nobili, Improving high-voltage cycling performance of nickel-rich NMC layered oxide cathodes for rechargeable Lithium–Ion batteries by Mg and Zr co-doping, Mater. Today Sustain. 20 (2022) 100236, http://dx.doi.org/10.1016/j.mtsust.2022.100236.

[67] S. El Moutchou, H. Aziam, M. Mansori, I. Saadoune, Thermal stability of Lithium-ion batteries: case study of NMC811 and LFP cathode materials, Mater. Today: Proc. 51 (2022) A1–A7, http://dx.doi.org/10.1016/j.matpr.2022.02.324.

[68] S.B. Peterson, J. Apt, J.F. Whitacre, Lithium-Ion battery cell degradation resulting from realistic vehicle and vehicle-to-grid utilization, J. Power Sources 195 (8) (2010) 2385–2392, http://dx.doi.org/10.1016/j.jpowsour.2009.10.010.

[69] Fastmarkets, The EV battery chemistry debate just got more complicated, 2022, https://www.fastmarkets.com/insights/the-ev-battery-chemistry-debate-just-got-more-complicated. (Accessed 22 August 2023).

[70] Battery University, BU-216: summary table of Lithium-based batteries, 2024, https://batteryuniversity.com/article/bu-216-summary-table-of-lithium-based-batteries. (Accessed 3 March 2025).

[71] L. Wildfeuer, A. Karger, D. Aygül, N. Wassiliadis, A. Jossen, M. Lienkamp, Experimental degradation study of a commercial Lithium-Ion battery, J. Power Sources 560 (2023) 232498, http://dx.doi.org/10.1016/j.jpowsour.2022.232498.

[72] M.-K. Tran, A. DaCosta, A. Mevawalla, S. Panchal, M. Fowler, Comparative study of equivalent circuit models performance in four common Lithium-Ion batteries: LFP, NMC, LMO, NCA, Batteries 7 (3) (2021) 51, http://dx.doi.org/10.3390/batteries7030051.

[73] SPGlobal, Batteries: Emerging chemistries create trade-offs in cost, performance, 2023, https://www.spglobal.com/marketintelligence/en/news-insights/latest-news-headlines/batteries-emerging-chemistries-create-trade-offs-in-cost-performance-75866899. (Accessed 17 August 2023).

[74] McKinsey, Lithium-Ion battery demand forecast for 2030 | McKinsey, 2023, https://www.mckinsey.com/industries/automotive-and-assembly/our-insights/battery-2030-resilient-sustainable-and-circular. (Accessed 24 October 2023).

[75] N. Kunanusont, T. Sesuk, P. Eiamlamai, S. Buakeaw, P. Tammawat, P. Limthongkul, Degradation diagnostics of Ni-rich NMC in Lithium-Ion Batteries Aged in different degrading conditions, ECS Meet. Abstr. MA2023-02 (3) (2023) 451, http://dx.doi.org/10.1149/MA2023-023451mtgabs.

[76] T. Wang, K. Ren, W. Xiao, W. Dong, H. Qiao, A. Duan, H. Pan, Y. Yang, H. Wang, Tuning the Li/Ni disorder of the NMC811 cathode by thermally driven competition between lattice ordering and structure decomposition, J. Phys. Chem. C 124 (10) (2020) 5600–5607, http://dx.doi.org/10.1021/acs.jpcc.0c00720.

[77] A. Eldesoky, N. Kowalski, J.R. Dahn, Highlighting the advantages of operating NMC811 cells to voltages below 4.20 V compared to NMC grades with lower Ni content, J. Electrochem. Soc. 170 (8) (2023) 080515, http://dx.doi.org/10.1149/1945-7111/aceffd.

[78] M.N. Naseer, J. Serrano-Sevillano, M. Fehse, I. Bobrikov, D. Saurel, Silicon anodes in Lithium-Ion batteries: A deep dive into research trends and global collaborations, J. Energy Storage 111 (2025) 115334, http://dx.doi.org/10.1016/j.est.2025.115334.

[79] C.-w. Liu, V. Lau, L.-y. Tsui, B.Q. Loo, H.-p. Hsu, C.-w. Lan, Exfoliability of two-dimensional silicon nanosheets from calcium disilicide and its enhanced performance as Lithium-Ion battery anode material, J. Energy Storage 72 (2023) 108399, http://dx.doi.org/10.1016/j.est.2023.108399.

[80] J.D. McBrayer, M.-T.F. Rodrigues, M.C. Schulze, D.P. Abraham, C.A. Apblett, I. Bloom, G.M. Carroll, A.M. Colclasure, C. Fang, K.L. Harrison, G. Liu, S.D. Minteer, N.R. Neale, G.M. Veith, C.S. Johnson, J.T. Vaughey, A.K. Burrell, B. Cunningham, Calendar aging of silicon-containing batteries, Nat. Energy 6 (9) (2021) 866–872, http://dx.doi.org/10.1038/s41560-021-00883-w.

[81] A. Zülke, Y. Li, P. Keil, R. Burrell, S. Belaisch, M. Nagarathinam, M.P. Mercer, H.E. Hoster, High-energy nickel-cobalt-aluminium oxide (NCA) cells on idle: Anode- versus cathode-driven side reactions, Batter. Supercaps 4 (6) (2021) 934–947, http://dx.doi.org/10.1002/batt.202100046.
[82] L. Yang, W. Deng, W. Xu, Y. Tian, A. Wang, B. Wang, G. Zou, H. Hou, W. Deng, X. Ji, Olivine LiMn x Fe 1-x PO 4 cathode materials for Lithium Ion batteries: Restricted factors of rate performances, J. Mater. Chem. A 9 (25) (2021) 14214–14232, http://dx.doi.org/10.1039/D1TA01526E.
[83] S. Li, H. Zhang, Y. Liu, L. Wang, X. He, Comprehensive understanding of structure transition in LiMnyFe1-yPO4 during delithiation/lithiation, Adv. Funct. Mater. (2023) 2310057, http://dx.doi.org/10.1002/adfm.202310057.
[84] U.-H. Kim, L.-Y. Kuo, P. Kaghazchi, C.S. Yoon, Y.-K. Sun, Quaternary layered Ni-rich NCMA cathode for Lithium-Ion batteries, ACS Energy Lett. 4 (2) (2019) 576–582, http://dx.doi.org/10.1021/acsenergylett.8b02499.
[85] F.B. Planella, W. Ai, A.M. Boyce, A. Ghosh, I. Korotkin, S. Sahu, V. Sulzer, R. Timms, T.G. Tranter, M. Zyskin, S.J. Cooper, J.S. Edge, J.M. Foster, M. Marinescu, B. Wu, G. Richardson, A continuum of physics-based Lithium-Ion battery models reviewed, Prog. Energy 4 (4) (2022) 042003, http://dx.doi.org/10.1088/2516-1083/ac7d31.
[86] W. Guo, Z. Sun, S.B. Vilsen, J. Meng, D.I. Stroe, Review of "Grey Box" lifetime modeling for Lithium-Ion battery: combining physics and data-driven methods, J. Energy Storage 56 (2022) 105992, http://dx.doi.org/10.1016/j.est.2022.105992.
[87] F. von Bülow, T. Meisen, A review on methods for state of health forecasting of Lithium-Ion batteries applicable in real-world operational conditions, J. Energy Storage 57 (2023) 105978, http://dx.doi.org/10.1016/j.est.2022.105978.
[88] J. Wang, P. Liu, J. Hicks-Garner, E. Sherman, S. Soukiazian, M. Verbrugge, H. Tataria, J. Musser, P. Finamore, Cycle-life model for graphite-LiFePO4 cells, J. Power Sources 196 (8) (2011) 3942–3948, http://dx.doi.org/10.1016/j.jpowsour.2010.11.134.
[89] J. de Hoog, J.-M. Timmermans, D. Ioan-Stroe, M. Swierczynski, J. Jaguemont, S. Goutam, N. Omar, J. Van Mierlo, P. Van Den Bossche, Combined cycling and calendar capacity fade modeling of a Nickel-Manganese-Cobalt Oxide Cell with real-life profile validation, Appl. Energy 200 (2017) 47–61, http://dx.doi.org/10.1016/j.apenergy.2017.05.018.
[90] E. Redondo-Iglesias, P. Venet, S. Pelissier, Calendar and cycling ageing combination of batteries in electric vehicles, Microelectron. Reliab. 88 (2018) 1212–1215.
[91] M. Broussely, Ph. Biensan, F. Bonhomme, Ph. Blanchard, S. Herreyre, K. Nechev, R.J. Staniewicz, Main aging mechanisms in Li Ion batteries, J. Power Sources 146 (1) (2005) 90–96, http://dx.doi.org/10.1016/j.jpowsour.2005.03.172.
[92] S.-h. Wu, P.-H. Lee, Storage fading of a commercial 18650 cell comprised with NMC/LMO cathode and graphite anode, J. Power Sources 349 (2017) 27–36, http://dx.doi.org/10.1016/j.jpowsour.2017.03.002.
[93] M.S. Hosen, D. Karimi, T. Kalogiannis, A. Pirooz, J. Jaguemont, M. Berecibar, J. Van Mierlo, Electro-aging model development of nickel-manganese-cobalt Lithium-Ion technology validated with light and heavy-duty real-life profiles, J. Energy Storage 28 (2020) 101265.
[94] T. Frambach, R. Liedtke, E. Figgemeier, Battery sizing of 48 V plug-in hybrids considering calendar and cycle degradation, J. Energy Storage 60 (2023) 106681.
[95] M. Naumann, M. Schimpe, P. Keil, H.C. Hesse, A. Jossen, Analysis and modeling of calendar aging of a commercial LiFePO4/Graphite cell, J. Energy Storage 17 (2018) 153–169.
[96] M. Schimpe, M.E. von Kuepach, M. Naumann, H.C. Hesse, K. Smith, A. Jossen, Comprehensive modeling of temperature-dependent degradation mechanisms in Lithium Iron phosphate batteries, J. Electrochem. Soc. 165 (2) (2018) A181, http://dx.doi.org/10.1149/2.1181714jes.
[97] X. Sui, M. Świerczyński, R. Teodorescu, D.-I. Stroe, The degradation behavior of LiFePO4/C Batteries during long-term calendar aging, Energies 14 (6) (2021) 1732, http://dx.doi.org/10.3390/en14061732.
[98] M. Dubarry, N. Qin, P. Brooker, Calendar aging of commercial Li-ion cells of different chemistries – A review, Curr. Opin. Electrochem. 9 (2018) 106–113, http://dx.doi.org/10.1016/j.coelec.2018.05.023.
[99] H.J. Ploehn, P. Ramadass, R.E. White, Solvent diffusion model for aging of Lithium-Ion battery cells, J. Electrochem. Soc. 151 (3) (2004) A456, http://dx.doi.org/10.1149/1.1644601.
[100] K. Liu, T.R. Ashwin, X. Hu, M. Lucu, W.D. Widanage, An evaluation study of different modelling techniques for calendar ageing prediction of Lithium-Ion batteries, Renew. Sustain. Energy Rev. 131 (2020) 110017, http://dx.doi.org/10.1016/j.rser.2020.110017.
[101] J. Wang, J. Purewal, P. Liu, J. Hicks-Garner, S. Soukazian, E. Sherman, A. Sorenson, L. Vu, H. Tataria, M.W. Verbrugge, Degradation of Lithium Ion batteries employing graphite negatives and nickel–cobalt–manganese oxide + spinel manganese oxide positives: Part 1, aging mechanisms and life estimation, J. Power Sources 269 (2014) 937–948, http://dx.doi.org/10.1016/j.jpowsour.2014.07.030.
[102] D.-I. Stroe, M. Swierczynski, S.K. Kær, R. Teodorescu, Degradation behavior of Lithium-Ion batteries during calendar ageing—The Case of the internal resistance increase, IEEE Trans. Ind. Appl. 54 (1) (2018) 517–525, http://dx.doi.org/10.1109/TIA.2017.2756026.
[103] J. Schmalstieg, S. Käbitz, M. Ecker, D.U. Sauer, A holistic aging model for Li(NiMnCo)O2 based 18650 Lithium-Ion batteries, J. Power Sources 257 (2014) 325–334, http://dx.doi.org/10.1016/j.jpowsour.2014.02.012.
[104] E. Sarasketa-Zabala, I. Gandiaga, E. Martinez-Laserna, L.M. Rodriguez-Martinez, I. Villarreal, Cycle ageing analysis of a LiFePO4/Graphite cell with dynamic model validations: Towards realistic lifetime predictions, J. Power Sources 275 (2015) 573–587, http://dx.doi.org/10.1016/j.jpowsour.2014.10.153.
[105] B. Xu, A. Oudalov, A. Ulbig, G. Andersson, D.S. Kirschen, Modeling of Lithium-Ion battery degradation for cell life assessment, IEEE Trans. Smart Grid 9 (2) (2018) 1131–1140, http://dx.doi.org/10.1109/TSG.2016.2578950.
[106] C. Guenther, B. Schott, W. Hennings, P. Waldowski, M.A. Danzer, Model-based investigation of electric vehicle battery aging by means of vehicle-to-grid scenario simulations, J. Power Sources 239 (2013) 604–610, http://dx.doi.org/10.1016/j.jpowsour.2013.02.041.
[107] L. Calearo, A. Thingvad, M. Marinelli, Modeling of battery electric vehicles for degradation studies, in: 2019 54th International Universities Power Engineering Conference, UPEC, 2019, pp. 1–6, http://dx.doi.org/10.1109/UPEC.2019.8893474.
[108] J. Olmos, I. Gandiaga, A. Saez-de-Ibarra, X. Larrea, T. Nieva, I. Aizpuru, Modelling the cycling degradation of Li-ion batteries: Chemistry influenced stress factors, J. Energy Storage 40 (2021) 102765, http://dx.doi.org/10.1016/j.est.2021.102765.
[109] J. Shim, K.A. Striebel, Cycling performance of low-cost Lithium Ion batteries with natural graphite and LiFePO4, J. Power Sources 119–121 (2003) 955–958, http://dx.doi.org/10.1016/S0378-7753(03)00297-0.
[110] W. Guo, Z. Sun, Y. Li, S.B. Vilsen, D.I. Stroe, How to identify mechanism consistency for LFP/C batteries during accelerated calendar and cycling aging using the lognormal distribution, in: 2023 IEEE Applied Power Electronics Conference and Exposition, APEC, IEEE, 2023, pp. 1816–1821.
[111] Y. Li, J. Guo, K. Pedersen, L. Gurevich, D.-I. Stroe, Investigation of multi-step fast charging protocol and aging mechanism for commercial NMC/Graphite Lithium-Ion batteries, J. Energy Chem. 80 (2023) 237–246, http://dx.doi.org/10.1016/j.jechem.2023.01.016.
[112] D.-I. Stroe, M. Swierczynski, A.-I. Stroe, R. Laerke, P.C. Kjaer, R. Teodorescu, Degradation behavior of Lithium-Ion batteries based on lifetime models and field measured frequency regulation mission profile, IEEE Trans. Ind. Appl. 52 (6) (2016) 5009–5018, http://dx.doi.org/10.1109/TIA.2016.2597120.
[113] T. Waldmann, M. Wilka, M. Kasper, M. Fleischhammer, M. Wohlfahrt-Mehrens, Temperature dependent ageing mechanisms in Lithium-ion batteries–A Post-Mortem study, J. Power Sources 262 (2014) 129–135.
[114] M. Schindler, J. Sturm, S. Ludwig, A. Durdel, A. Jossen, Comprehensive analysis of the aging behavior of Nickel-rich, Silicon-Graphite Lithium-Ion cells subject to varying temperature and charging profiles, J. Electrochem. Soc. 168 (6) (2021) 060522.
[115] F. Richter, P.J. Vie, S. Kjelstrup, O.S. Burheim, Measurements of ageing and thermal conductivity in a secondary NMC-hard carbon Li-ion battery and the impact on internal temperature profiles, Electrochim. Acta 250 (2017) 228–237.
[116] K. Jalkanen, J. Karppinen, L. Skogström, T. Laurila, M. Nisula, K. Vuorilehto, Cycle aging of commercial NMC/Graphite pouch cells at different temperatures, Appl. Energy 154 (2015) 160–172, http://dx.doi.org/10.1016/j.apenergy.2015.04.110.
[117] N. Omar, M.A. Monem, Y. Firouz, J. Salminen, J. Smekens, O. Hegazy, H. Gaulous, G. Mulder, P. Van den Bossche, T. Coosemans, et al., Lithium Iron phosphate based battery–Assessment of the aging parameters and development of cycle life model, Appl. Energy 113 (2014) 1575–1585.
[118] M. Simolka, J.F. Heger, H. Kaess, I. Biswas, K.A. Friedrich, Influence of cycling profile, depth of discharge and temperature on commercial LFP/C cell ageing: Post-mortem material analysis of structure, morphology and chemical composition, J. Appl. Electrochem. 50 (11) (2020) 1101–1117, http://dx.doi.org/10.1007/s10800-020-01465-6.
[119] L. Su, J. Zhang, C. Wang, Y. Zhang, Z. Li, Y. Song, T. Jin, Z. Ma, Identifying main factors of capacity fading in Lithium Ion cells using orthogonal design of experiments, Appl. Energy 163 (2016) 201–210.
[120] D. Hu, G. Chen, J. Tian, N. Li, L. Chen, Y. Su, T. Song, Y. Lu, D. Cao, S. Chen, et al., Unrevealing the effects of low temperature on cycling life of 21700-type cylindrical Li-ion batteries, J. Energy Chem. 60 (2021) 104–110.
[121] A. Krupp, R. Beckmann, T. Diekmann, G. Liebig, E. Ferg, F. Schuldt, C. Agert, Semi-empirical cyclic aging model for stationary storages based on graphite anode aging mechanisms, J. Power Sources 561 (2023) 232721.
[122] Y. Gao, J. Jiang, C. Zhang, W. Zhang, Y. Jiang, Aging mechanisms under different state-of-charge ranges and the multi-indicators system of state-of-health for Lithium-Ion battery with Li (NiMnCo) O2 cathode, J. Power Sources 400 (2018) 641–651.
[123] M. Ecker, N. Nieto, S. Käbitz, J. Schmalstieg, H. Blanke, A. Warnecke, D.U. Sauer, Calendar and cycle life study of Li (NiMnCo) O2-based 18650 Lithium-Ion batteries, J. Power Sources 248 (2014) 839–851, http://dx.doi.org/10.1016/j.jpowsour.2013.09.143.
[124] J. Jiang, W. Shi, J. Zheng, P. Zuo, J. Xiao, X. Chen, W. Xu, J.-G. Zhang, Optimized operating range for large-format LiFePO4/Graphite batteries, J. Electrochem. Soc. 161 (3) (2013) A336.

[125] F. Benavente-Araoz, M. Varini, A. Lundblad, S. Cabrera, G. Lindbergh, Effect of partial cycling of NCA/Graphite cylindrical cells in different SoC intervals, J. Electrochem. Soc. 167 (4) (2020) 040529, http://dx.doi.org/10.1149/1945-7111/ab78fd.

[126] S. Lee, L. Su, A. Mesnier, Z. Cui, A. Manthiram, Cracking vs. Surface reactivity in high-nickel cathodes for Lithium-Ion batteries, Joule 7 (11) (2023) 2430–2444, http://dx.doi.org/10.1016/j.joule.2023.09.006.

[127] S. Barcellona, L. Piegari, Effect of current on cycle aging of Lithium Ion batteries, J. Energy Storage 29 (2020) 101310, http://dx.doi.org/10.1016/j.est.2020.101310.

[128] X. Chen, Y. Hu, S. Li, Y. Wang, D. Li, C. Luo, X. Xue, F. Xu, Z. Zhang, Z. Gong, et al., State of health (SoH) estimation and degradation modes analysis of pouch NMC532/Graphite Li-ion battery, J. Power Sources 498 (2021) 229884, http://dx.doi.org/10.1016/j.jpowsour.2021.229884.

[129] W. Xie, R. He, X. Gao, X. Li, H. Wang, X. Liu, X. Yan, S. Yang, Degradation identification of LiNi0. 8Co0. 1Mn0. 1o2/Graphite Lithium-Ion batteries under fast charging conditions, Electrochim. Acta 392 (2021) 138979.

[130] S. Sun, T. Guan, X. Cheng, P. Zuo, Y. Gao, C. Du, G. Yin, Accelerated aging and degradation mechanism of LiFePO 4/Graphite batteries cycled at high discharge rates, RSC Adv. 8 (45) (2018) 25695–25703.

[131] M. Naumann, F.B. Spingler, A. Jossen, Analysis and modeling of cycle aging of a commercial LiFePO4/Graphite cell, J. Power Sources 451 (2020) 227666, http://dx.doi.org/10.1016/j.jpowsour.2019.227666.

[132] Y. Preger, H.M. Barkholtz, A. Fresquez, D.L. Campbell, B.W. Juba, J. Romàn-Kustas, S.R. Ferreira, B. Chalamala, Degradation of commercial Lithium-Ion cells as a function of chemistry and cycling conditions, J. Electrochem. Soc. 167 (12) (2020) 120532, http://dx.doi.org/10.1149/1945-7111/abae37.

[133] D. Cui, J. Wang, A. Sun, H. Song, W. Wei, Anomalously faster deterioration of $LiNi_{0.8}Co_{0.15}Al_{0.05}O_2$/graphite high-energy 18650 cells at 1.5 C than 2.0 C, Scanning 2018 (2018) e2593780, http://dx.doi.org/10.1155/2018/2593780.

[134] A. Maheshwari, M. Heck, M. Santarelli, Cycle aging studies of lithium nickel manganese cobalt oxide-based batteries using electrochemical impedance spectroscopy, Electrochim. Acta 273 (2018) 335–348, http://dx.doi.org/10.1016/j.electacta.2018.04.045.

[135] S. Watanabe, M. Kinoshita, T. Hosokawa, K. Morigaki, K. Nakura, Capacity fading of LiAlyNi1- x- yCoxO2 cathode for Lithium-Ion batteries during accelerated calendar and cycle life tests (effect of depth of discharge in charge–discharge cycling on the suppression of the micro-crack generation of LiAlyNi1- x- yCoxO2 particle), J. Power Sources 260 (2014) 50–56.

[136] G. He, Q. Chen, C. Kang, P. Pinson, Q. Xia, Optimal bidding strategy of battery storage in power markets considering performance-based regulation and battery cycle life, IEEE Trans. Smart Grid 7 (5) (2016) 2359–2367, http://dx.doi.org/10.1109/TSG.2015.2424314.

[137] S. Englberger, H. Hesse, D. Kucevic, A. Jossen, A techno-economic analysis of vehicle-to-building: battery degradation and efficiency analysis in the context of coordinated electric vehicle charging, Energies 12 (5) (2019) 955, http://dx.doi.org/10.3390/en12050955.

[138] C.N. Truong, M. Naumann, R.C. Karl, M. Müller, A. Jossen, H.C. Hesse, Economics of residential photovoltaic battery systems in Germany: The case of Tesla's powerwall, Batteries 2 (2) (2016) 14, http://dx.doi.org/10.3390/batteries2020014.

[139] M.S. Carmeli, N. Toscani, M. Mauri, Electrothermal aging model of Li-Ion batteries for vehicle-to-grid services evaluation, Electronics 11 (7) (2022) 1042, http://dx.doi.org/10.3390/electronics11071042.

[140] H.-G. Lee, J.-W. Choi, S.-T. Ryu, K.-J. Lee, Life degradation of Lithium-Ion batteries under vehicle-to-grid operations based on a multi-physics model, Int. J. Automot. Technol. 26 (2) (2025) 315–326, http://dx.doi.org/10.1007/s12239-024-00157-w.

[141] J. Gong, D. Wasylowski, J. Figgener, S. Bihn, F. Rücker, F. Ringbeck, D.U. Sauer, Quantifying the impact of V2X operation on electric vehicle battery degradation: An experimental evaluation, ETransportation 20 (2024) 100316, http://dx.doi.org/10.1016/j.etran.2024.100316.

[142] R. Khezri, D. Steen, E. Wikner, L.A. Tuan, Optimal V2G scheduling of an EV with calendar and cycle aging of battery: An MILP approach, IEEE Trans. Transp. Electrification (2024) http://dx.doi.org/10.1109/TTE.2024.3384293, 1–1.

[143] H. Movahedi, S. Pannala, J. Siegel, S.J. Harris, D. Howey, A. Stefanopoulou, Extra throughput versus days lost in V2G services: Influence of dominant degradation mechanism, J. Energy Storage 104 (2024) 114242, http://dx.doi.org/10.1016/j.est.2024.114242.

[144] Y. Zheng, Z. Shao, X. Lei, Y. Shi, L. Jian, The economic analysis of electric vehicle aggregators participating in energy and regulation markets considering battery degradation, J. Energy Storage 45 (2022) 103770, http://dx.doi.org/10.1016/j.est.2021.103770.

[145] J.A. Manzolli, J.P.F. Trovão, C. Henggeler Antunes, Electric bus coordinated charging strategy considering V2G and battery degradation, Energy 254 (2022) 124252, http://dx.doi.org/10.1016/j.energy.2022.124252.

[146] Y. He, B. Venkatesh, L. Guan, Optimal scheduling for charging and discharging of electric vehicles, IEEE Trans. Smart Grid 3 (3) (2012) 1095–1105, http://dx.doi.org/10.1109/TSG.2011.2173507.

[147] S. Li, P. Zhao, C. Gu, J. Li, S. Cheng, M. Xu, Online battery protective energy management for energy-transportation nexus, IEEE Trans. Ind. Inform. 18 (11) (2022) 8203–8212, http://dx.doi.org/10.1109/TII.2022.3163778.

[148] Q. Badey, G. Cherouvrier, Y. Reynier, J. Duffault, S. Franger, Ageing forecast of lithium-ion batteries for electric and hybrid vehicles, 2012.

[149] A. Thingvad, L. Calearo, P.B. Andersen, M. Marinelli, Empirical capacity measurements of electric vehicles subject to battery degradation from V2G services, IEEE Trans. Veh. Technol. 70 (8) (2021) 7547–7557, http://dx.doi.org/10.1109/TVT.2021.3093161.

[150] G. Baure, M. Dubarry, Durability and reliability of EV batteries under electric utility grid operations: Impact of frequency regulation usage on cell degradation, Energies 13 (10) (2020) 2494, http://dx.doi.org/10.3390/en13102494.

[151] R. Das, Y. Wang, G. Putrus, R. Kotter, M. Marzband, B. Herteleer, J. Warmerdam, Multi-objective techno-economic-environmental optimisation of electric vehicle for energy services, Appl. Energy 257 (2020) 113965, http://dx.doi.org/10.1016/j.apenergy.2019.113965.

[152] M. Sufyan, N.A. Rahim, M.A. Muhammad, C.K. Tan, S.R.S. Raihan, A.H.A. Bakar, Charge coordination and battery lifecycle analysis of electric vehicles with V2G implementation, Electr. Power Syst. Res. 184 (2020) 106307, http://dx.doi.org/10.1016/j.epsr.2020.106307.

[153] C. Zhou, K. Qian, M. Allan, W. Zhou, Modeling of the cost of EV battery wear due to V2G Application in power systems, IEEE Trans. Energy Convers. 26 (4) (2011) 1041–1050, http://dx.doi.org/10.1109/TEC.2011.2159977.

[154] A. Ahmadian, M. Sedghi, A. Elkamel, M. Fowler, M. Aliakbar Golkar, Plug-in electric vehicle batteries degradation modeling for smart grid studies: review, assessment and conceptual framework, Renew. Sustain. Energy Rev. 81 (2018) 2609–2624, http://dx.doi.org/10.1016/j.rser.2017.06.067.

[155] M. Dubarry, A. Devie, K. McKenzie, Durability and reliability of electric vehicle batteries under electric utility grid operations: Bidirectional charging impact analysis, J. Power Sources 358 (2017) 39–49, http://dx.doi.org/10.1016/j.jpowsour.2017.05.015.

[156] J. Witt, EV battery health after 250 million electric car miles, 2023, https://www.recurrentauto.com/research/lessons-in-electric-car-battery-health.

[157] M. Jafari, A. Gauchia, S. Zhao, K. Zhang, L. Gauchia, Electric vehicle battery cycle aging evaluation in real-world daily driving and vehicle-to-grid services, IEEE Trans. Transp. Electrification 4 (1) (2018) 122–134, http://dx.doi.org/10.1109/TTE.2017.2764320.

[158] J.-O. Lee, Y.-S. Kim, Novel battery degradation cost formulation for optimal scheduling of battery energy storage systems, Int. J. Electr. Power Energy Syst. 137 (2022) 107795, http://dx.doi.org/10.1016/j.ijepes.2021.107795.

[159] G. Luo, Y. Zhang, A. Tang, Capacity degradation and aging mechanisms evolution of Lithium-Ion Batteries under different operation conditions, Energies 16 (10) (2023) 4232, http://dx.doi.org/10.3390/en16104232.

[160] C.F. Calvillo, K. Czechowski, L. Söder, A. Sanchez-Miralles, J. Villar, Vehicle-to-grid profitability considering EV battery degradation, in: 2016 IEEE PES Asia-Pacific Power and Energy Engineering Conference, APPEEC, 2016, pp. 310–314, http://dx.doi.org/10.1109/APPEEC.2016.7779518.

[161] M.M. Rahman, E. Gemechu, A.O. Oni, A. Kumar, The development of a techno-economic model for assessment of cost of energy storage for vehicle-to-grid applications in a cold climate, Energy 262 (2023) 125398, http://dx.doi.org/10.1016/j.energy.2022.125398.